

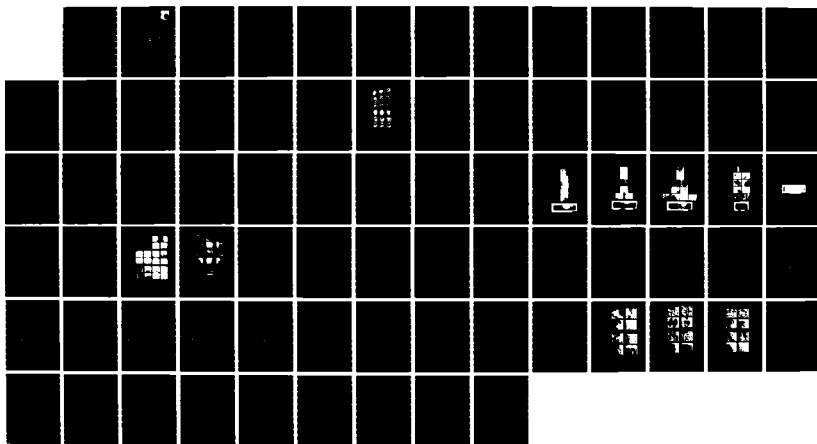
RD-A168 884

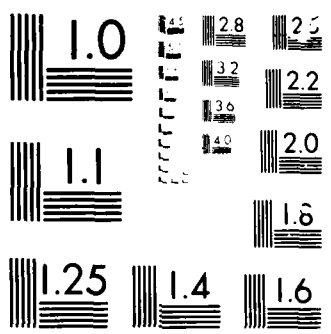
IMPROVEMENT IN DUCTILITY AND FRACTURE TOUGHNESS OF
HIP'D AND ISOTHERMALLY. (U) AIR FORCE WRIGHT

1/1

AERONAUTICAL LABS WRIGHT-PATTERSON AFB OH

UNCLASSIFIED R P SIMPSON ET AL. JUN 86 AFWAL-TR-86-4864 F/G 11/6 NL





MURKIN 4

44-27

AD-A168 804

AFWAL-TR-86-4064

IMPROVEMENT IN DUCTILITY AND FRACTURE
TOUGHNESS OF HIP'1 AND ISOTHERMALLY FORGED
Ti-6Al-6V-2Sn POWDER WITH HEAT TREATMENT



Schmid P. Simpson, Lt Col, USAF
Metals Branch
Manufacturing Technology Division

Attwell M. Adair
Metals Branch
Manufacturing Technology Division

Francis H. Gross
Structural Metals Branch
Metals and Ceramics Division

Daniel E. Jen
University of Dayton
Dayton, Ohio

JUN 17 1986

DTIC
ELECTED
JUN 17 1986
S *[Handwritten Signature]* **D**

Final Report for Period June 1979 to June 1986

Approved for Public Release; Distribution Unlimited

WRIGHT LABORATORY
AF WRIGHT AERONAUTICAL LABORATORIES
AF SYSTEMS COMMAND
WRIGHT-PATTERSON AFB OH 45433-6653

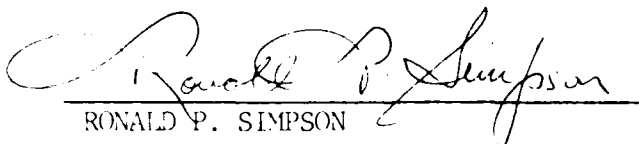
82 611 019

NOTICE

When Government drawings, specifications, or other data are used for any purpose other than in connection with a definitely related Government procurement operation, the United States Government thereby incurs no responsibility nor any obligation whatsoever; and the fact that the government may have formulated, furnished, or in any way supplied the said drawings, specifications, or other data, is not to be regarded by implication or otherwise as in any manner licensing the holder or any other person or corporation, or conveying any rights or permission to manufacture use, or sell any patented invention that may in any way be related thereto.

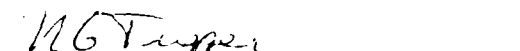
This report has been reviewed by the Office of Public Affairs (ASD/PA) and is releasable to the National Technical Information Service (NTIS). At NTIS, it will be available to the general public, including foreign nations.

This technical report has been reviewed and is approved for publication.


RONALD P. SIMPSON


ATTWELL M. ADAIR

FOR THE COMMANDER


NATHAN G. TIPPER
Acting Director
Manufacturing Technology Division

"If your address has changed, if you wish to be removed from our mailing list, or if the addressee is no longer employed by your organization please notify AEWAL/MLTM, W-PAFB, OH 45433 to help us maintain a current mailing list".

Copies of this report should not be returned unless return is required by security considerations, contractual obligations, or notice on a specific document.

UNCLASSIFIED

SECURITY CLASSIFICATION OF THIS PAGE

REPORT DOCUMENTATION PAGE

1a REPORT SECURITY CLASSIFICATION Unclassified		1b. RESTRICTIVE MARKINGS	
2a. SECURITY CLASSIFICATION AUTHORITY		3. DISTRIBUTION/AVAILABILITY OF REPORT Approved for public release, distribution unlimited	
2b DECLASSIFICATION/DOWNGRADING SCHEDULE			
4 PERFORMING ORGANIZATION REPORT NUMBER(S) AFWAL-TR-86- 4 064		5. MONITORING ORGANIZATION REPORT NUMBER(S)	
6a NAME OF PERFORMING ORGANIZATION AF Wright Aeronautical Laboratories, Materials Lab	6b. OFFICE SYMBOL (If applicable) AFWAL/MLTM	7a. NAME OF MONITORING ORGANIZATION	
6c. ADDRESS (City, State and ZIP Code) Wright-Patterson AFB OH 45433-6533		7b. ADDRESS (City, State and ZIP Code)	
8a NAME OF FUNDING/SPONSORING ORGANIZATION	8b. OFFICE SYMBOL (If applicable)	9. PROCUREMENT INSTRUMENT IDENTIFICATION NUMBER F33615-73-C-5092*	
8c. ADDRESS (City, State and ZIP Code)		10. SOURCE OF FUNDING NOS.	
		PROGRAM ELEMENT NO. 62102F	PROJECT NO. 2418
11. TITLE (Include Security Classification) Improvement in Ductility and Fracture Toughness of HIP'D (See reverse)		TASK NO.	WORK UNIT NO.
12. PERSONAL AUTHORISI Ronald P. Simpson, Attwell M. Adair, Francis H. Froes, Daniel Eylon			
13a. TYPE OF REPORT Final	13b. TIME COVERED FROM Jun 78 TO Jun 86	14. DATE OF REPORT (Yr., Mo., Day) 86/June	15. PAGE COUNT 76
16. SUPPLEMENTARY NOTATION *In part			
17. COSATI CODES		18. SUBJECT TERMS (Continue on reverse if necessary and identify by block number) Heat Treatment Fracture Surfaces Powder Metallurgy Electron Microscopy Hot Isostatic Pressing Metals Processing Mechanical Properties Hot Die Forging	
19. ABSTRACT (Continue on reverse if necessary and identify by block number) This program was aimed at optimizing the mechanical behavior of powder metallurgy compacts of the Ti-6Al-6V-2Sn alloy. Particular emphasis was placed on breaking-up continuous grain boundary alpha which previous work had indicated was detrimental to the properties of concern, particularly ductility and fracture toughness. A range of microstructures were produced in Hydride-Dehydride and Rotating Electrode Powder Compacts using combinations of hot isostatic pressing, extrusion, isothermal forging and heat treatment. Based on the microstructural studies, two heat treatments were selected and used in combination with powder compaction (Hot isostatic pressing or extrusion) and isothermal forging to develop mechanical properties which were correlated with processing, microstructure and fractographic features. Two types of microstructures were identified as having acceptable levels of strength, ductility and fracture toughness: (1) a high volume fraction of fine equiaxed primary alpha in a matrix of transformed beta and (2) a relatively coarse secondary alpha plate dispersion in combination with a small volume fraction of large low aspect (See reverse)			
20. DISTRIBUTION/AVAILABILITY OF ABSTRACT UNCLASSIFIED UNLIMITED <input checked="" type="checkbox"/> SAME AS RPT <input type="checkbox"/> DTIC USERS <input type="checkbox"/>		21. ABSTRACT SECURITY CLASSIFICATION Unclassified	
22a. NAME OF RESPONSIBLE INDIVIDUAL R.P. Simpson		22b. TELEPHONE NUMBER (Include Area Code) 513-255-2413	22c. OFFICE SYMBOL AFWAL/MLTM

Item 11 cont'd

and Isothermally Forged Ti-6Al-6V-2Sn with Heat Treatment

Item 19 cont'd

ratio primary alpha. The processing routes necessary to develop structures were defined.

PREFACE

This final technical report covers work conducted by Lt Col Ronald P. Simpson during the time period June 1978 to June 1986 under the USAF Reserve Program, AFWAL Materials Laboratory, Wright Patterson AFB, Ohio 45433. Lt Col Simpson is Vice President of Marketing and Sales for Amdata Corporation, San Jose, CA, a wholly owned subsidiary of Combustion Engineering, Windsor Locks, CT.

The work was performed under the technical direction of Mr. A.M. Adair, formerly of the Processing and High Temperature Materials Branch, Metals and Ceramics Division (AFWAL/MLLM), now with the Metals Branch, Manufacturing Technology Division (AFWAL/MLTM), Wright-Patterson AFB, Ohio 45433. The authors are also very grateful to several other persons who contributed significantly to this overall program including Dr. I. Martorell, M. Myers, T. Jones, R. Sweeney, T. Brown, and J. Brown, for processing the alloy billets; S. Boone, V. Vidoni, G. Teeters, for metallographic assistance; C. Heidenreich, for photographic assistance; J. Paine, for mechanical testing and graphic arts ; C. Cook and R. Burdecki for scanning electron microscopy (SEM).

The alloy billets used for this program were provided by Nuclear Metals Inc., Concord, Massachusetts under Contract No. F33615-73-C-5092 with the Materials Laboratory.

Accession For	
NTIS	CRA&I
DTIC	TAB
Unannounced	
Justification	
By _____	
Distribution / _____	
Availability Codes	
Dist	Avail and/or Special
A-1	



TABLE OF CONTENTS

SECTION		PAGE
I	INTRODUCTION	1
II	EXPERIMENTAL PROCEDURE	3
	1. Phase I - Microstructure Study	4
	2. Phase II - Mechanical Property Study	7
	3. Process Description	8
	a. Powder Production	8
	b. Powder Compaction	12
	c. Isothermal Forging	15
	d. Heat Treatment	17
	e. Metallurgical Evaluation	17
	f. Mechanical Testing	18
	g. Fractographic Evaluation	22
III	RESULTS and DISCUSSION	24
	1. Phase I - Microstructure Study	25
	a. Microstructure Development	31
	b. Heat Treatment Selection for Phase II	32
	2. Phase II - Mechanical Property Study	32
	a. Microstructure Development	35
	b. Microstructure Interpretation	36
	c. Mechanical Properties	39
	d. Fractography	52
	e. Correlation of Microstructure, Mechanical Properties and Fractography	58
IV	CONCLUSIONS	63

REFERENCES

LIST OF ILLUSTRATIONS

FIGURE		PAGE
1	Diagram of Phase I and Phase II Procedure - Sequences of Thermo-mechanical Processing.	5/6
2	Photograph of 20 Sectioned Billets.	9
3	Rotating Electrode Powder (REP) Powder-Making Apparatus.	11
4	Schematic of Sample Removal for Isothermal Forged (IF) Billet Heat Treatment Study in Phase I of Program.	19
5	Tensile Sample Sketch with Dimensions.	20
6	Charpy Sample Sketch with Dimensions.	21
7	Effect of Heat Treatments on Microstructures of Hydride-Dehydride (HDH) Powder Below T_B	26
8	Effect of Heat Treatments on Microstructures of Rotating Electrode Powder HIP'd Below T_B	27
9	Effect of Heat Treatments on Microstructures of Hydride-Dehydride Powder HIP'd Above T_B	28
10	Effect of Heat Treatments on Microstructures of Rotating Electrode Powder HIP'd Above T_B	29
11	Effect of IF and Subsequent Heat Treatment (HT) (Three Step) on Microstructure of Rotating Electrode Powder HIP'd Below T_B	30
12	Ti-6Al-6V-2Sn Compacted Powder Microstructures.... for Heat Treating (HT1) Conditions.	33

LIST OF ILLUSTRATIONS - Continued

FIGURE		PAGE
13	Ti-6Al-6V-2Sn Compacted Powder Microstructures.... for Heat Treating (HT2) Conditions.	34
14	Ductility as measured by Reduction of Area (RA) as a function of YS for 20 conditions as detailed in Figure 1b.	42
15	Ductility as measured by elongation as a function of YS for 20 conditions detailed in Figure 1b.	43
16	Fracture toughness as measured by K_Q as a function of YS for 20 conditions detailed in Figure 1b.	44
17	Fracture toughness as measured by K_V (calculated from Work per unit Area (W/A)) as a function of YS for 20 conditions detailed in Figure 1b.	45
18	Fracture toughness as measured by Work per unit Area as a function of Y.S. for 20 conditions detailed in Figure 1b.	46
19	Ductility as measured by Reduction of Area as a function of UTS for 20 conditions as detailed in Figure 1b.	47
20	Ductility as measured by elongation as a function of UTS for 20 conditions detailed in Figure 1b.	48
21	Fracture toughness as measured by K_Q as a function of UTS for 20 conditions detailed in Figure 1b.	49
22	Fracture toughness as measured by K_V (calculated from Work per unit Area) as a function of UTS for 20 conditions detailed in Figure 1b.	50

LIST OF ILLUSTRATIONS - Continued

FIGURE	PAGE
23	Fracture toughness as measured by Work per unit Area as a function of UTS for 20 conditiond detailed in Figure 1b. 51
24	Ti-6Al-6V-2Sn Tensile and Charpy V-Notch Fractographs --- Hydride-Dehydride (HDH) Powder --- Conditions #4 and #7. 55
25	Ti-6Al-6V-2Sn Tensile and Charpy V-Notch Fractographs --- Rotating Electrode (REP) Powder --- Conditions #24 and #27. ... 56
26	Ti-6Al-6V-2Sn Tensile and Charpy V-Notch Fractographs --- Rotating Electrode (REP) Powder --- Conditions #3 and #22. ... 57

LIST OF TABLES

TABLE		PAGE
1	Density of Ti-6Al-6V-2Sn Powders	14
2	Peak Loads During Isothermal Forging for Each Sample Condition ..	16
3	Summary of Microstructure and Property Features of the Six Samples Chosen for Fractographic Analysis	23
4	Proximity of Each Thermo-Mechanical Process Step to the Beta Transus Temperature (°F)	35
5	Ti-6Al-6V-2Sn Compacted Powder Sample Thermo-Mechanical Treatment and Mechanical Properties	41
6	Microstructure Class Designation with Sample Number and UTS	58
7	Microstructure Classification of the Tested Conditions	59
8	Property Correlation to Alpha Morphology	60

SECTION I

INTRODUCTION

As the design of aircraft engines becomes more advanced, requiring increased performance and efficiency, the need for materials which can withstand higher stresses and temperatures is also increased. This need for improved mechanical properties has led to the development of higher-strength titanium alloys which can be achieved through alloy additions and careful control of processing. The higher strength, however, is obtained at the cost of increased alloy complexity. Higher alloy additions increase the difficulties involved in melting and hot working, contributing to the tendency for non-uniformity of properties of cast and wrought products. Control of the microstructure and chemical homogeneity, therefore becomes more difficult when applying conventional cast and wrought technology to advanced alloys (1, 2, 3).

Powder metallurgy (PM) offers a potential solution to the chemical homogeneity problem by restricting segregation both because of the small size of the individual particles and the more rapid solidification rate of some PM processes. This then provides chemical- and mechanical-property homogeneity (2). This technology also provides a means of fabricating near-net-shape components either by HIPing to shape or fabrication of precision forging preform shapes (4 - 13).

For more than fifteen years the AFWAL Materials Laboratory (AFWAL/ML) has invested in the development of advanced manufacturing technology to exploit the economic and technical advantages of near-net-shape components (14), particularly by reducing machining, labor and material usage. The latter factor also has strategic advantages in the case of certain critical alloying additions.

The PM approach also has the capability to distribute stresses more uniformly during compaction and to give a product with little or no texture (8), resulting in more uniform residual stresses and microstructures. Hence, parts can be produced having superior, more consistent mechanical properties.

Strength, ductility, and toughness can be increased and non-uniformities in properties associated with forming operations reduced (15, 16).

The advantages of PM and near-net-shape technology (17) can be combined with wrought microstructural features utilizing the hot isostatic press (HIP) compaction of powders followed by isothermal forging (IF) of the preform-shaped compact to a near-net-shape component. Three important advantages are: (8, 17, 19)

1. Achievement of homogeneous structures for complex alloys having a favorable morphology associated with the forging process.
2. Signification material savings.
3. Manufacturing cost reduction opportunities.

Earlier AFWAL/ML-sponsored work with Ti-6Al-6V-2Sn powders (20) investigated the effect of HIP and IF upon the structure and properties of both Hydride-Dehydride (HDH) and Rotating Electrode Process (REP) powders. The results showed a reduction in toughness and ductility over a conventionally forged, wrought product for the same alloy. Subsequent annealing treatment improved toughness but did not alter the ductility or strength. This low ductility was probably a result of the continuous grain boundary alpha which is detrimental to ductility in alloys of this class (21). The objective of the current program was to develop alternative heat treatments which would improve ductility and/or toughness without reducing strength. Success was achieved with a similar program for post weld heat treatments of Ti-6Al-6V-2Sn (21). Heat treatments developed during this earlier weldment work formed the basis for the current post HIP + IF property improvement studies. The thrust of the present program is therefore to investigate the capability of fully dense PM, in combination with IF and innovative heat treatments, to achieve high levels of mechanical properties in the Ti-6Al-6V-2Sn alloy.

SECTION II

EXPERIMENTAL PROCEDURE

1. Phase I - Microstructure Study
2. Phase II - Mechanical Property Study
3. Process Description
 - a. Powder Production
 - b. Powder Compaction
 - c. Isothermal Forging
 - d. Heat Treatment
 - e. Metallurgical Evaluation
 - f. Mechanical Testing
 - g. Fractographic Evaluation

SECTION II

EXPERIMENTAL PROCEDURE

A two phase program was designed to develop a heat treatment that will increase toughness and/or ductility of isothermally forged (IF) Ti-6Al-6V-2Sn HIP'd powder compacts. A schematic outline of each phase is given in Figure 1. The first phase was a metallurgical structure study, Figure 1a, to evaluate the effect of heat treatments on microstructure. Three heat treatments were evaluated; two of these were selected for Phase II of the study, mechanical property evaluation, Figure 1b.

1. PHASE I - MICROSTRUCTURE STUDY

Three heat treatments were designed to break up the continuous grain-boundary α phase and elongated α in Phase I of this program. This α phase morphology is known to result in lower ductility and toughness in Ti-6Al-6V-2Sn and other two phase titanium alloys (21). Each of the three heat treatments was used on two types of powder, Hydride-Dehydride (HDH) and Rotating Electrode Process (REP) powders. In all six process and thermal-cycle conditions were metallurgically evaluated by optical microscopy as follows: (The beta transus temperature of Ti-6Al-6V-2Sn is typically 1705°F).

1. HIP [1630°F (890°C)/15ksi/2hr]
2. HIP + Vacuum Anneal [1450°F (790°C) 2hr/FC to 1000°F/AC (540°C)].
3. HIP + IF [1650°F (900°C)/50%/0.3 ipm (7.6mm/min) AC]
4. HIP + IF + AN [1450°F (790°C) 2hr/FC to 1000°F (540°C)/AC].
5. HIP + IF + STA [1650°F (900°C) 1/2hr + WQ/1050°F (566°C) 24hr/AC].
6. HIP + IF + H.T. [1350°F (730°C) 6hr/AC + 1680°F (915°C) 3hr/AC + 1350°F (730°C) 3hr/AC].

Microstructures were characterized at 100X and 400X. Heat treatments in both Conditions 5 and 6 were selected for Phase II based on the criteria that they refine the α phase morphology and break up the continuous grain-boundary α phase. They are designated HT1 and HT2 respectively in Phase II. For the same reason, the all β HIPed material was not selected for Phase II in deference to $\alpha + \beta$ HIPed (1630°F (890°C)] powders.

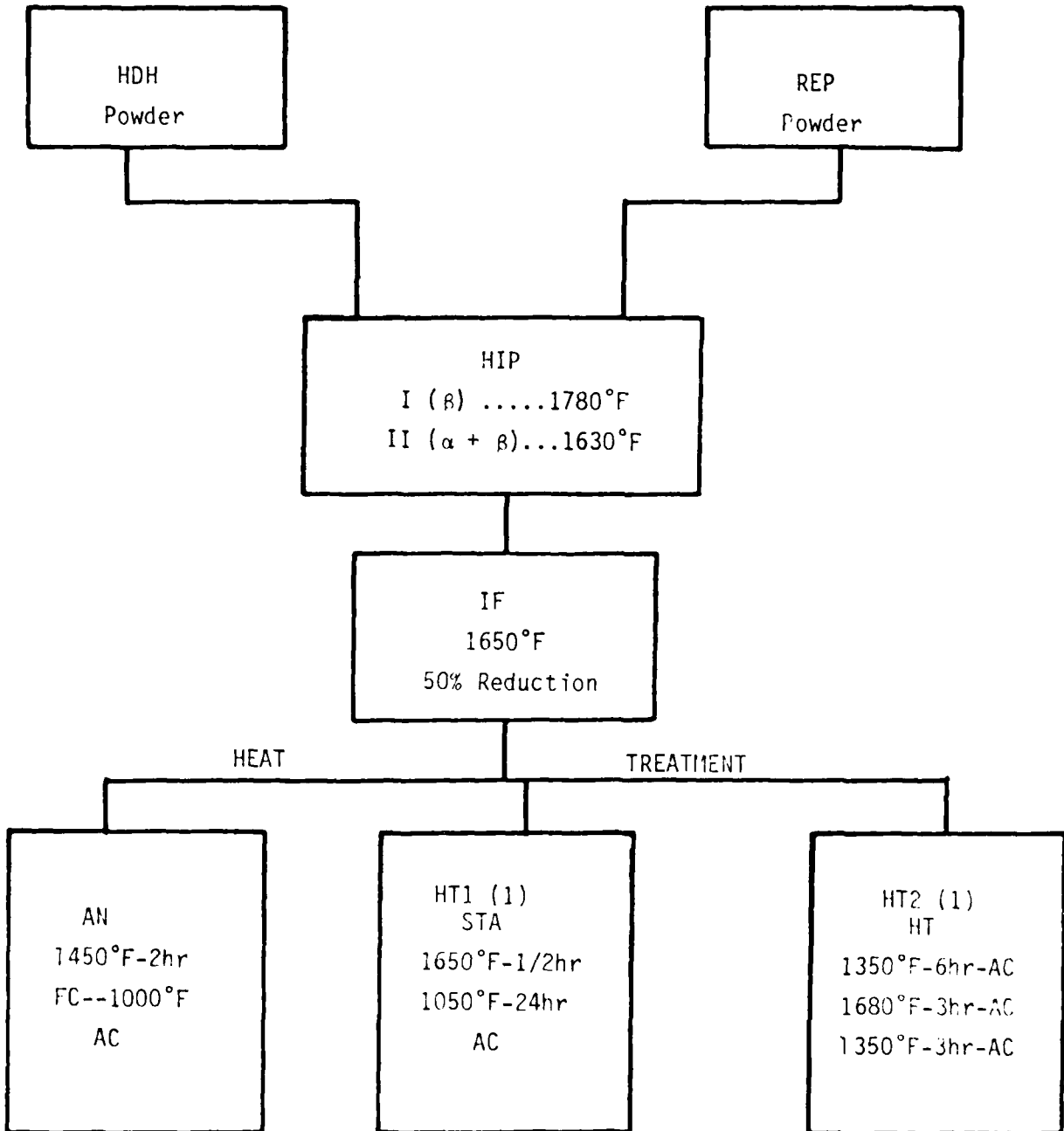


Figure 1(a). PHASE I - Metallurgical Structure Evaluation Sequence of Thermo-Mechanical Processing

(1) Designation used in Phase II

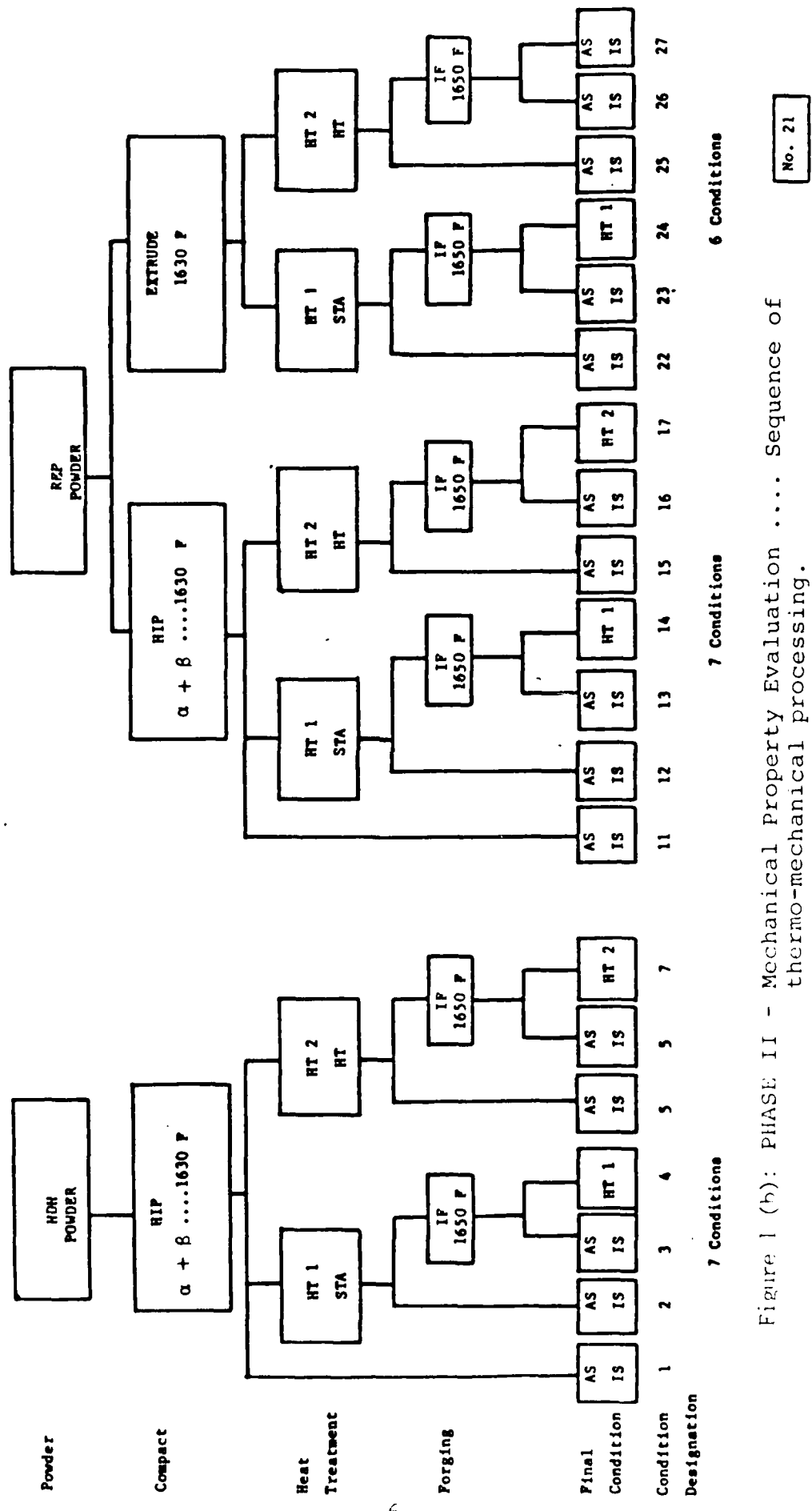


Figure 1 (b): PHASE II - Mechanical Property Evaluation Sequence of thermo-mechanical processing.

2. PHASE II - MECHANICAL PROPERTY STUDY

The two most promising heat treatments from microstructure observations were applied to compacted powder (HDH powder by HIP'ing and REP powder by both HIP'ing and extruding) to evaluate their effect on mechanical properties. Billets for each of these three conditions were treated as follows:

1. Heat treated by both HT1 (Condition 5) and HT2 (Condition 6).
2. Isothermally forged (IF).
3. Re-heat treated (HT1 and HT2).

The sequence of steps for each of the three starting material conditions is demonstrated in Figure 1b. Note the numbering sequence is consistent for each of the three conditions. Since as-extruded material was not available for testing and characterization, there is no sample 21. The same pattern is seen in Figure 2 where each of the 20 billets is arranged by powder type, heat treatment and process sequence. The sample numbering scheme is consistent with the thermal-mechanical processing sequence depicted in Figure 1b.

The numbering scheme is also carried through all tables and Figures used to present test results. Note that a sample billet was preserved for each of the two heat treatments and each of the three-powder production/compaction combinations at each of the three process stages, yielding a total of $2 \times 3 \times 3 = 18$ samples.

In addition, as HIP'd billets were included for both HDH and REP powder, making a total of 20 sample conditions (7 HDH and HIPed, 7 REP and HIPed, 6 REP and extruded). As-extruded material was not available for testing and characterization.

Heat-treatment effectiveness was evaluated through tensile and fracture-toughness tests as well as microstructural characterization and fractographic analysis. After the various heat-treatments and isothermal-forging sequences were complete, each of the 20 billets was cut in half, and two blanks were removed for tensile samples (R3 type with 1-in. gage length), Figure 5 and two for low-bend precracked Charpy fracture toughness samples, Figure 6.. In addition,

macro-characterization was completed on each of the 20 billets to demonstrate metal flow during working, and samples were removed for microstructural characterization at the center and the edge of each billet, both perpendicular and parallel to the forging direction (cylindrical axis). The photograph in Figure 2 shows the final processed billets after completion of all sectioning.

3. PROCESS DESCRIPTION

Details of the specific procedures for each of the seven major process operations follow:

1. Powder Production
 2. Powder Compaction (Hot Isostatic Pressing and Extrusion)
 3. Isothermal Forging
 4. Heat Treatment
 5. Metallurgical Evaluation
 6. Mechanical Testing
 7. Fractographic Evaluation
- a. Powder Production

Two types of powder manufacturing techniques were utilized in this study:

1. Hydride-Dehydride (HDH), and
2. Rotating Electrode Process (REP)

Care was taken to make the powders chemically homogenous and impurity free.

(1) HDH Process

In the Hydride-Dehydride (HDH) Process, a titanium bar is heated and then cooled in a hydrogen atmosphere to convert it to the friable metal hydride. The hydride is then crushed to a powder and subsequently heated in vacuum, whereupon it is converted to a metal powder once again in a somewhat sintered state. The sintered cake is broken up and the powder passed through a magnetic separator to remove steel particles from the attritor. The powder has

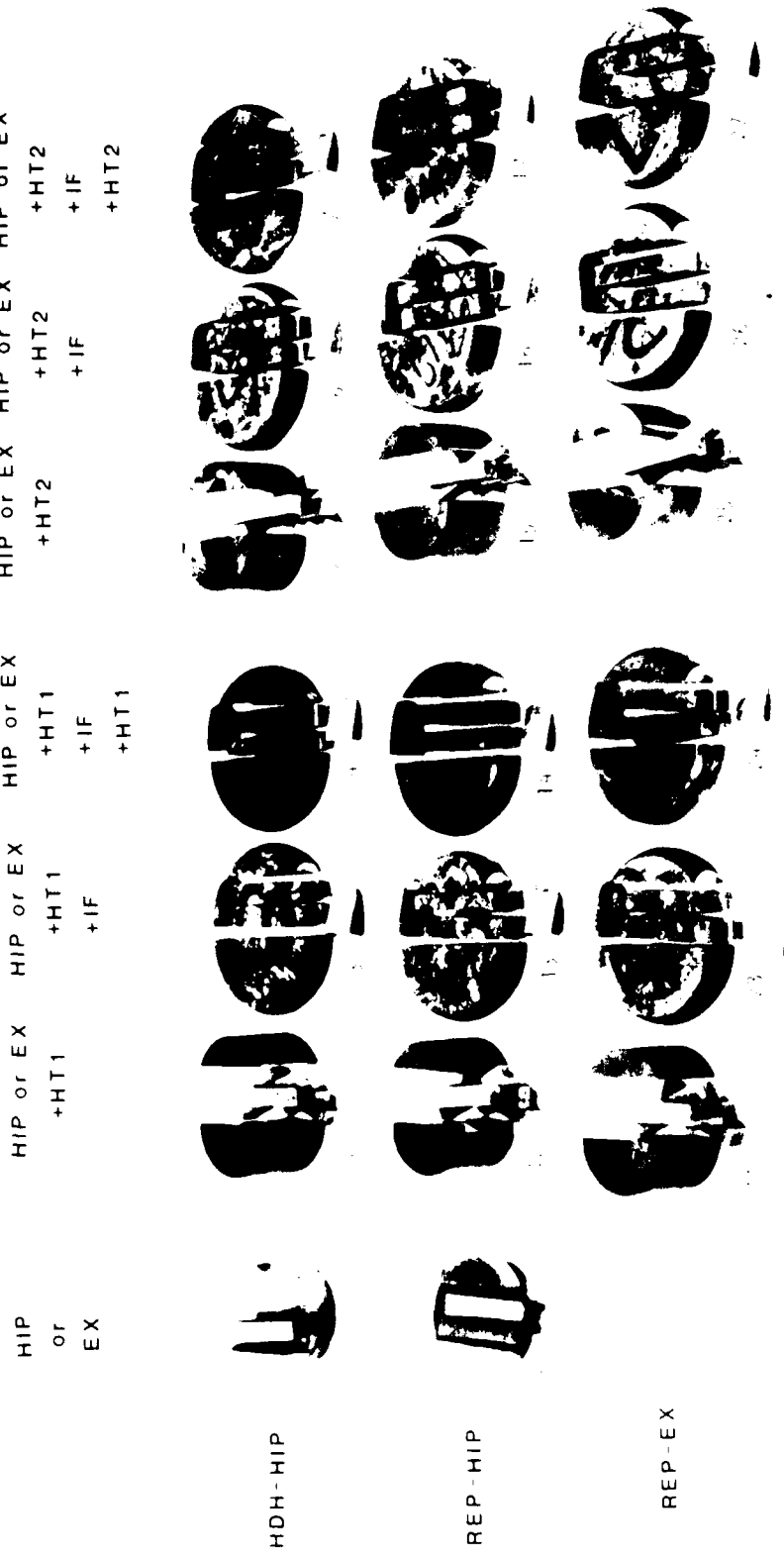


Figure 2: Photographs of HIP and IF billets made from Ti-6Al-6V-2Sn powder. Both HHDH (top row) and REP (middle and bottom rows) powders were used. Initial powder compaction was accomplished by hot isostatic pressing (top two rows), and extrusion (bottom row). Arrangement follows identification sequence in left of Table 2. Each row is different powder/compaction combination. Each group of three columns represents a different heat treatment, HT1 (left), HT2 (right). Two samples on far left are as-HIPped compacted of HHDH powder (top) and REP powder (middle). As-extruded REP powder sample not available. Each billet was sectioned to provide two tensile, and two Charpy sample blanks as well as material for metallographic examination.

a flaky angular appearance and has bulk and tap densities in the range 35-45% of theoretical.

The powder produced by this technique is less pure than REP powder, with respect to both interstitial elements and metal species originating in the crushing apparatus. It also has a lower tap density and at the time of the purchase it was more expensive than titanium alloy powder made by the Rotating Electrode Process. Due to the angular morphology it has sufficient green strength to permit cold compaction in either a die or isostatic press.

(2) REP Process

Powder is produced in the Rotating Electrode Process (REP) by arc melting the face of a rapidly rotating alloy electrode bar. The consumable rotating alloy electrode and a non-consumable tungsten electrode are contained within a large chamber which has been evacuated and then filled with helium (Figure 3). As the consumable electrode rotates, centrifugal force causes the molten metal to fly off in the form of fine droplets that solidify in flight into spherical microcastings. A current modification to the REP process utilizes a plasma torch instead of a tungsten electrode ("PREP") resulting in a higher overall quality product. Powder particle size is controlled by the electrode diameter and the speed at which the electrode is rotated; a typical titanium electrode is 2-1/2 in. (63mm) in diameter. Since the rotating electrode is melted in the absence of a crucible and since melting takes place in a high-purity static gas atmosphere, the powder produced is of very high purity, the chemical analysis being similar to that of the starting material. This process was developed and patented by Nuclear Metals, Inc. (NMI). The REP powder particles are predominantly smooth spheres, with an average particle size of 200-250 ; virtually no particles finer than 325 mesh (44). The spherical powder cannot be cold compacted at room temperature.

The bulk (loose) density of REP titanium powder is typically 60-62% of theoretical and the powder can be vibrated to a tap density of 64-66% of theoretical.

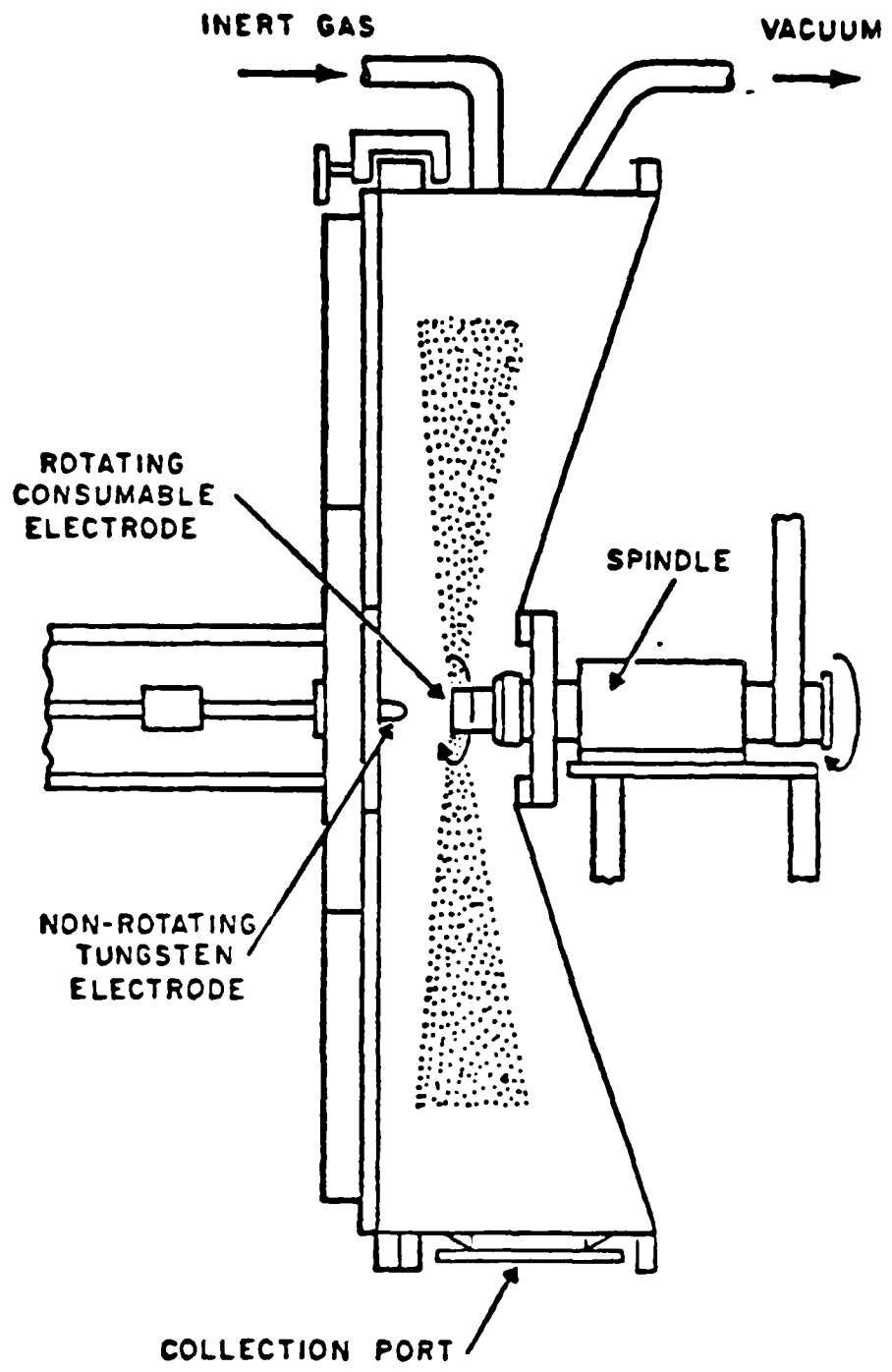


Figure 3: REP Powder-Making Apparatus.

Pre-alloyed powders used in this study were obtained and consolidated into HIP or extruded billets in an earlier study (1). A complete description of observations and results of the powder production and evaluation process is given in that reference along with a comprehensive analysis of powder chemistry, particle size distribution, surface characterization, density, and metallographic structure.

5. Powder Compaction

Both HDH and REP powders were separated into two particle sizes: -35 mesh and -60 + 200 mesh [1]. While the smooth-surface spherical REP powders had a much higher tap density than the rough angular HDH powders, there was very little difference in tap density of the two mesh sizes, as seen in Table 1. Also in the previous study [1] no difference in mechanical properties was found for the different particle size cut compacts. A variation in properties for the HDH powder compacts after HIPing was observed, but it was not consistent and showed no trend attributable to particle size (1). All REP powder compacts exhibited consistent, uniform properties. Consequently, only the -35 mesh powder compacts were used in this heat-treatment study. The REP powder was compacted by extruding as well as HIPing.

(1) Hot Isostatic Pressing

The REP powder, because its tap density (TD) was 64% of theoretical, was poured into the HIP cannisters, tapped, evacuated, outgassed at 300°F (149°C) to remove any absorbed air or moisture on the powder or on the can interior, and sealed. The cannisters were made of seamless carbon steel tubes, 3.56-in. (90.4mm) ID X 0.095-in. (2.5mm) wall X 4-1/2 in. (114.3mm) inside height.

The HDH powder, even after tapping, was only 46-50% dense. Uncompensated, this 50% porosity would result in an undersized billet of non-uniform dimensions and, because of the larger deformation which a billet would undergo in the HIP autoclave, it possibly could result in a ruptured can weld. Therefore, the HDH powder was preconsolidated to approximately 67% TD by

isostatic compaction at room temperature. This was accomplished by pouring the powder into a rubber bag and tapping, after which the bag was evacuated, sealed, and pressurized in water at 25ksi. These cold-compacted billets were then loaded into steel cans and processed as noted above, except that outgassing was conducted at 1000°F (538°C). The lower REP powder outgassing temperature was used because the powder manufacturers (NMI) experience with the REP powder, which was reinforced by the present work, shows that little outgassing occurs between 70 and 300°F and none occurs above that temperature.

HIP consolidation of the two powder types was performed at 1630°F (890°C) at 15ksi for 2hr. The billets were compacted in a conventional autoclave at Industrial Materials Technology (IMT) in Woburn, MA. In the IMT processing, the billets are heated by a furnace within the autoclave and pressurized by argon. This procedure was selected from a variety of times, pressures, and temperatures evaluated and reported in Ref. 1. Little variation in mechanical properties was observed with HIP process variables, even for temperature. Consolidation time and pressure are factors deemed to have more of an economic than a physical significance, to the extent that similar properties are obtained. This was demonstrated in the previous work with a range of times extending from under 1/2 hr to 4 hrs and pressures of 3.75, 7.5, and 15 ksi. The consolidation temperatures chosen were 75°F (24°C) above and below the β transus of 1705°F (930°C), in order to compare the effects of β vs $\alpha + \beta$ processing. Billets HIP'd for 2 hrs at 15ksi were selected as starting material for the present study. In Phase I both the 1630 and 1780°F (890 and 970°C) HIP'ing temperature billets were evaluated. Phase II was limited to the $\alpha + \beta$ HIP'd 1630°F (890°C) material since it produces a finer duplex microstructure which will yield superior properties.

(2) Extrusion

REP powders were extruded in a Brush-Wellman 2000-ton press at 50 in./min. (2ipm) through a 3.29 in. (4.6cm) die ($R = 6.24:1$) at 1630°F (890°C). The starting "billet" was made for extrusion by joining four 1018 steel cans together, each 8 in. (20.3cm) in diam. X 23 in. (58.4cm) long. Each can was filled, evacuated, outgassed at 300°F, (150°C) and welded. The extrusion force ranged from 2200 to 2600 tons.

TABLE 1
DENSITY OF Ti-6Al-6V-2Sn POWDERS

	ABSOLUTE DENSITY g/cm ³ (1b/in ³)		RELATIVE DENSITY (%)*	
	REP	HDH	REP	HDH
	-35 -60+200	-35 -60+200	-35 -60+200	-35 -60+200
Particle Density (Helium-Air Pycnometer)	4.51 (0.163)	4.59 (0.166)	4.51 (0.163)	4.59 (0.166)
Bulk Density (ASTM-B212-64)	2.63 (0.095)	2.72 (0.098)	1.67 (0.060)	1.62 (0.058)
Tap Density (ASTM-R527-70)	2.91 (0.104)	2.90 (0.105)	2.25 (0.081)	2.08 (0.075)

*With respect to wrought-bar density = 4.516 g/cm³ (0.163 lb/in³)
From Ref. 1.

After extrusion the steel jackets were removed by pickling in a dilute nitric-acid solution. The finished titanium extrusion was 24 ft. long and measured 2.930-3.040 in. (74.4-77.3 mm) in diam. The bar was machined into 48 pieces, each 2.925 in. (74.3mm) (or larger) in diam., X 6 in. long. Two of these 6-in. billets were starting material for the present heat-treatment investigation.

c. Isothermal Forging

Two 6-in. (15.2cm) long billets were available for each of the three powder compaction (P/C) conditions (HDH-HIP, REP-HIP, REP-EX). Each of these was sectioned and machined into three forging discs 2-in. in height having true, parallel faces. This provided six discs for each of the three P/C conditions. Three of each were given heat treatment 1 (HT1) and three of each received heat treatment 2 (HT2) as follows:

1. 1650°F (900°C)/1hr/WQ+1050°F (565°C)/24hr/AC
2. 1350°F (730°C)/6hr/AC+1680°F (915°C)/3hr/AC+1350°F (730°C)/3hr/AC

One billet was retained after heat treatment for each of the six P/C-HT combinations. Two of each were preheated to 1650°F (900°C), held for 45 minutes, and isothermally forged at a ram speed of 0.3 ipm with polygraph lubricant. In summary, the IF conditions were:

Reduction in Height	50%
Work Piece and Die Temperature	1650°F (900°C)
Preheating Time	45 Min.
Ram Speed	0.3 In./Min (.6mm/Min.)
Lubricant	Polygraph
Cooling Rate After Forging	Air Cool

Since the purpose of the forging was to assess the effect of the prior HIP and extrusion cycles upon forged material, the forging parameters were kept constant for all billets. Peak loads for each condition are given in Table 2.

TABLE 2

Peak Loads During Isothermal Forging for Each Sample Condition

Sample	Powder	Billet Condition	Isothermal Force Peak Load (Tons)
1	HDH	HIP	--
-	"	HIP+IF*	--
2	"	HIP+HT #1	--
3	"	HIP+HT #1+IF	53
4	"	HIP+HT #1+IF+HT #1	56
5	"	HIP+HT #2	--
6	"	HIP+HT #2+IF	48
7	"	HIP+HT #2+IF+HT #2	47
11	REP	HIP	--
-	"	HIP+IF*	--
12	"	HIP+HT #1	--
13	"	HIP+HT #1+IF	45
14	"	HIP+HT #1+IF+HT #1	43
15	"	HIP+HT #2	--
16	"	HIP+HT #2+IF	42
17	"	HIP+HT #2+IF+HT #2	42
(21)	REP	Extruded (not evaluated)	
22	"	Ex+HT #1	--
23	"	Ex+HT+IF	41
24	"	Ex+HT #1+IF+HT #1	42
25	"	Ex+HT #2	--
26	"	Ex+HT #2+IF	39
27	"	Ex+HT #2+IF+HT #2	38

One of the two billets IF for each of the two heat treatments was re-heat treated after forging. This sequence is shown in the arrangement of billets in Figure 2.

d. Heat Treatment

Heat treatments have been used successfully in the past in case of Ti-6Al-6V-2Sn to improve ductility and fracture toughness of weldments by breaking up and refining the continuous grain-boundary α network found during welding (2). That same continuous grain-boundary α phase is thought to be responsible for the low ductility and toughness of the Ti-6Al-6V-2Sn material (21). Consequently, similar heat treatments were designed in attempts to and produce the same beneficial effect in the processed powder billets.

In Phase I of this investigation, three thermal cycles were evaluated, on both powder types, compacted below and above the beta transus. The heat treatments were as follows:

1. STA [1650°F (900°C) 1/2hr/WQ+1050°F (565°C) 24hr/AC]
2. HT [1350°F (730°C) 6hr/AC+1680°F (915°C) 3hr/AC+1350°F (730°C)
3hr/AC]
3. AN [1450°F (790°C) 2hr/FC to 1000°F (540°C)/AC]

The HIP'ing conditions evaluated were $\alpha + \beta$ [1630°F (890°C), 15ksi 2hr], and all β [1780°F (970°C), 15ksi, 2hr].

Heat treatments 1 (HT1 in Phase II) and 2 (HT2 in Phase II) were carried out in a small Harrop furnace controlled within $\pm 10^{\circ}\text{F}$. Samples were protected from oxidation by wrapping them in stainless-steel bags containing titanium sponge as a getter. The annealing heat treatment was conducted in a vacuum environment.

e. Metallographic Evaluation

Metallographic samples were prepared in a conventional mount with a mechanical polishing technique. The microstructures were developed and examined with Krolls etchant and a Zeiss metallograph. Macrostructures were also etched

with Krolls etch and photographed by means of conventional photography. The sketch in Figure 4 shows locations where metallographic samples were removed and oriented for examination.

f. Mechanical Testing

Two tensile and two slow bend Charpy V-notched toughness samples were removed from each compacted billet as shown photographically in Figure 1. Tensile tests were performed on 0.252-in. gage diameter round specimens with threaded ends which were machined in accordance with ASTM-E8, as shown in Figure 5. Tests were run at room temperature on an Instron machine at a crosshead rate of 0.05 in./in./min.

The toughness of these PM billets was measured using slow bend pre-cracked Charpy specimens, Figure 6. The samples were pre-cracked in fatigue using a Universal fatigue machine operating at 30 Hz. The fatiguing was initiated at an alternating load of 100 to 800 lb. and was decreased for the last 0.050-in. of fatigue crack to 50-450 lb, which is equivalent to a ΔK of less than 20ksi in.

The pre-cracked Charpy bars were tested in three-point bending over a span of 1.6 in. (4.1cm). A load-displacement record was kept for each test; the energy absorbed in breaking the specimen was measured and reduced to energy (W) per unit area (A) of uncracked ligament. Hence, the units of toughness measurement were in.-lbs-per square inch, W/A. Fracture toughness was calculated from these W/A values using the following formula:

$$K_v^2 = \left[\frac{W}{A} \frac{E}{2(1-\nu^2)} \right]$$

$$E = \text{Youngs Modulus} = 16.5 \times 10^6$$

$$\nu = \text{Poissons Ratio} = 0.3$$

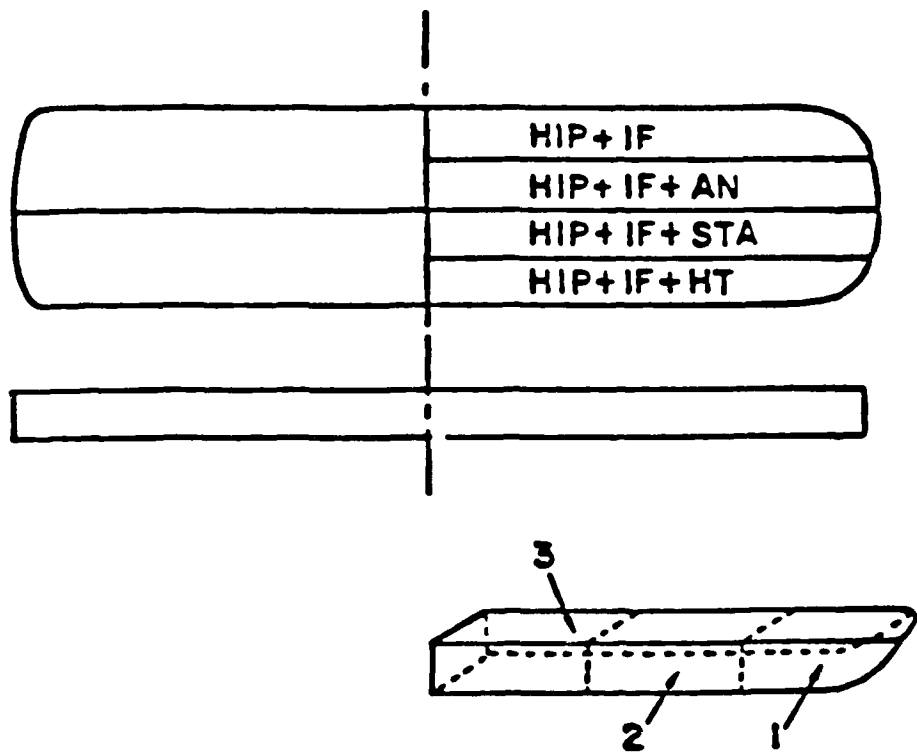
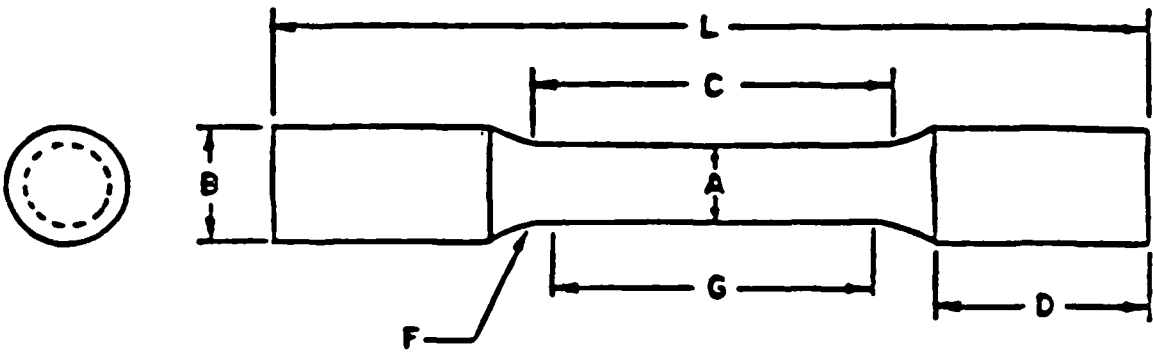


Figure 4. Schematic Representation of Method of Removal of Metallographic Samples from Isothermal Forging. In some instances both longitudinal and transverse sections were examined from Area 2. This is the most highly worked portion of the forged billet. Location 1 is a "dead" zone and receives little deformation during forging. Location 3 is in between. In some instances all three locations were examined.



DIMENSIONS (in.)	R3 (FORMERLY TYPE 4)
A- DIAMETER AT CENTER	0.252 ± 0.005
B- DIAMETER OF GRIP END APPROX.	$3/8$
C- LENGTH OF REDUCED SECTION, MIN.	$1 \frac{1}{4}$
D- GRIP LENGTH, APPROX.	$5/8$
F- FILLET RADIUS, MIN.	0.18
G- GAGE LENGTH	1.0 ± 0.005
L- TOTAL LENGTH, APPROX.	3
AREA OF CROSS SECTION, SQ. IN., APPROX.	$1/20$

Figure 5. Schematic Diagram and Dimensional Tolerances for ASTM Tensile Specimens. The R3 sample was used in the recent work.

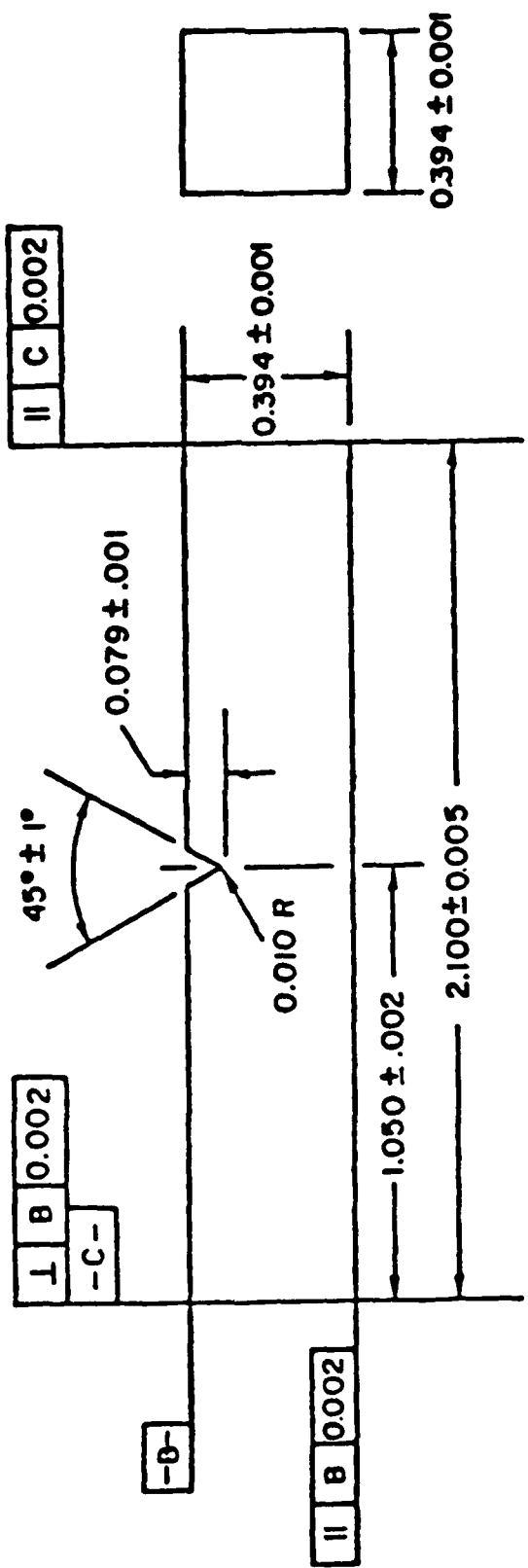


Figure 6. Schematic Diagram of Charpy V-Notch Fracture Toughness Sample.

Example Calculation:

Sample 1: $\frac{W}{A} = 308 \frac{\text{in-lb}}{\text{in}}$

$$\begin{aligned}K_v &= 308 \frac{16.5}{2(0.91)} \\&= (308) (9.066) \\K_v &= 53 \text{ ksi-in}^{\frac{1}{2}}\end{aligned}$$

Both W/A and K_v are given in Table 5 along with K_Q .

g. Fractographic Evaluation

Six microstructures (Table 3) were selected for fracture surface evaluation by scanning electron microscopy (SEM). One tensile and one fracture toughness sample were examined for each of samples 3,4,7,22,24 and 27. These sample conditions were selected to cover each of the major microstructures and property ranges and to cover similar process conditions for comparison of HT1 and HT2. For example samples 4 and 7 and samples 24 and 27 received HT2, at the same time 4 and 24 are in comparable process history conditions except 4 and 24 received HT1 while 7 and 27 received HT2. At the same time 4 and 24 are comparable since they have the identical thermo-mechanical history only 4 is HDH and 24 is REP powder. The very same comparison exists between samples 7 and 27.

Sample 3 was chosen because it has good strength and is on the high end of all mechanical properties measured in this work. It is considered to be a condition with a good combination of properties, is similar in microstructure to sample 7 but has better properties.

Sample 22 was selected because it represents the finest equiaxed microstructure obtained in this work, possibly recrystallized. The entire structure is fine, fully equiaxed. Consequently it is a high strength and relatively high fracture toughness and ductility condition.

A summary of the microstructure and property feature of the six samples chosen is given in Table 3.

TABLE 3

SUMMARY OF MICROSTRUCTURE AND PROPERTY FEATURES OF THE SIX
SAMPLES CHOSEN FOR FRACTOGRAPHIC ANALYSIS

<u>SAMPLE NUMBER</u>	<u>FEATURES (MICROSTRUCTURE and PROPERTIES)</u>
3	Lenticular - equiaxed structure Good combination of microstructural features leading to Good combination of properties
4	Very fine fully transformed δ lenticular microstructure with some coarser lenticular primary α Most susceptible to defect if any present HDH comparison to No. 24 --- low combination of properties
7	Equiaxed microstructure with some coarse primary Compare to No. 4 --- HT2 vs. HT1 Also compare to No. 3 --- similar microstructure
22	Fully equiaxed fine microstructure-possibly recrystallized Condition with highest amount of equiaxed α High Strength --- good toughness and ductility
24	Fine transformed δ lenticular microstructure with some primary coarser equiaxed α Similar to Pratt & Whitney commercially used Duplex Annealed Structure in the near alpha titanium alloys Good combination of properties High strength with good ductility and fracture toughness
27	Fully lenticular alpha structure --- colony structure Coarse transformed structure is low in ductility and low in strength Best in fracture toughness --- low strength

SECTION III

RESULTS and DISCUSSION

1. Phase I - Microstructure Study
 - a. Microstructure Development
 - b. Heat Treatment Selection for Phase II
2. Phase II - Mechanical Property Study
 - a. Microstructure Development
 - b. Microstructure Interpretation
 - c. Mechanical Properties
 - d. Fractography
 - e. Correlation of Microstructure, Mechanical Properties and Fractography

SECTION III

RESULTS

Very different microstructures and, therefore, mechanical properties are produced in Ti-6Al-6V-2Sn with variations in thermal-mechanical treatment. Earlier investigation showed a loss in ductility and toughness after isothermally forging powders compacted by HIPing and extruding (20) probably as a result of extensive grain boundary alpha (21). Success in overcoming such deficiencies in as welded structures of Ti-6Al-6V-2Sn (22) led to a similar program on these HIP'd and IF compacts. Results are presented for Phase I and Phase II separately. Many process conditions were examined in three heat treatment conditions in Phase I. The objective was to select the best heat treatment and compaction process conditions for property structure evaluation in Phase II.

1. PHASE I - MICROSTRUCTURE STUDY

In the first phase of the study structures were created by five process conditions.

1. HIP
2. HIP + IF
3. HIP + IF + AN
4. HIP + IF + STA.... becomes HT1 in Phase II
5. HIP + IF + HT.... becomes HT2 in Phase II

For two powders (REP and HDH) and for two HIPing conditions ($\alpha + \beta$ and β) are presented in Figures 7-10. These figures also show the macrostructure of the is-forged ingot. There is a large difference between the material HIP'd in the $\alpha + \beta$ region and the all β HIP'd ingot. The latter has large prior β grains and a much coarser microstructure. This difference can be seen by comparing Figures 7 and 8 to 9 and 10.

The macrostructures show "dead-zone" regions of the forging where there is little metal flow or deformation. In these regions there are relatively large and equiaxed grains having a coarser, underformed α phase. In contrast, the more highly worked zones show no evidence of a grain structure at all; and the α

EFFECT OF HEAT TREATMENT ON Ti-6Al-6V-2Sn POWDER MICROSTRUCTURES

HYDRIDE + DEHYDRIDE POWDER

HIPped 750 F Below Beta Transus (1630 F)

AS HIPed

HIP & IF

HIP & IF & AN

HIP & IF & STA

HIP & IF & HT

HIPped

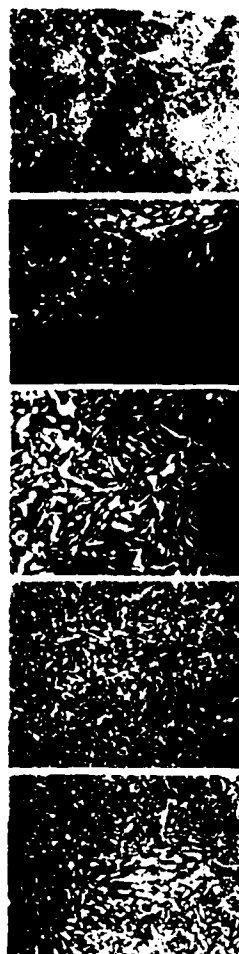


Figure 7.

EFFECT OF HEAT TREATMENT ON Ti-6Al-6V-2Sn POWDER MICROSTRUCTURES

ROTATING ELECTRODE POWDER
HIPed 75 F Below BetaTransus (1630 F)

AS-HIPed



HIP & F



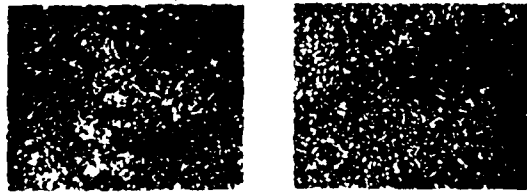
HIP & F & AN



HIP & F & STA



HIP & F & HT



(a)

(b)

HIP & F



Fig. 2.

EFFECT OF HEAT TREATMENT ON Ti-6Al-6V-2Sn POWDER MICROSTRUCTURES

HYDRIDE / DEHYDRIDE POWDER
HIPed 75 F Above Beta Transus (1780 F)

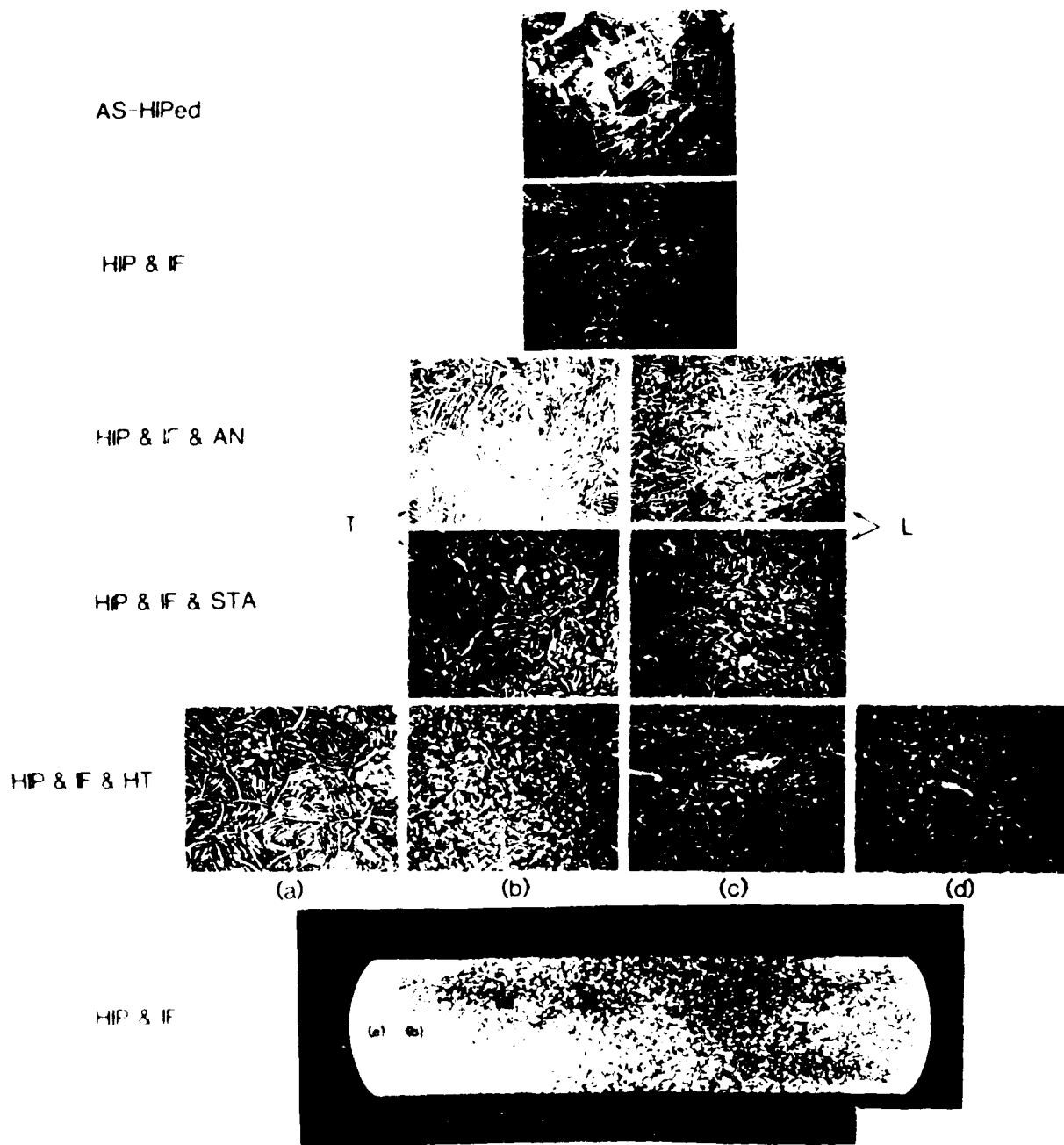


Figure 9.

EFFECT OF HEAT TREATMENT ON Ti-6Al-6V-2Sn POWDER MICROSTRUCTURES

ROTATING ELECTRODE POWDER

HIPed 75 F Above Beta Transus (1780 F)

AS HIPed



HIP & IF

(b)

(c)

HIP & IF & AN

T

L

HIP & IF & STA

(a)

(b)

(c)

HIP & IF & HT



Figure 10.

EFFECT OF ISOTHERMAL FORGING AND SUBSEQUENT
THREE STEP HEAT TREATMENT ON Ti-6Al-6V-2Sn
HIP_{ed} POWDER MICROSTRUCTURE

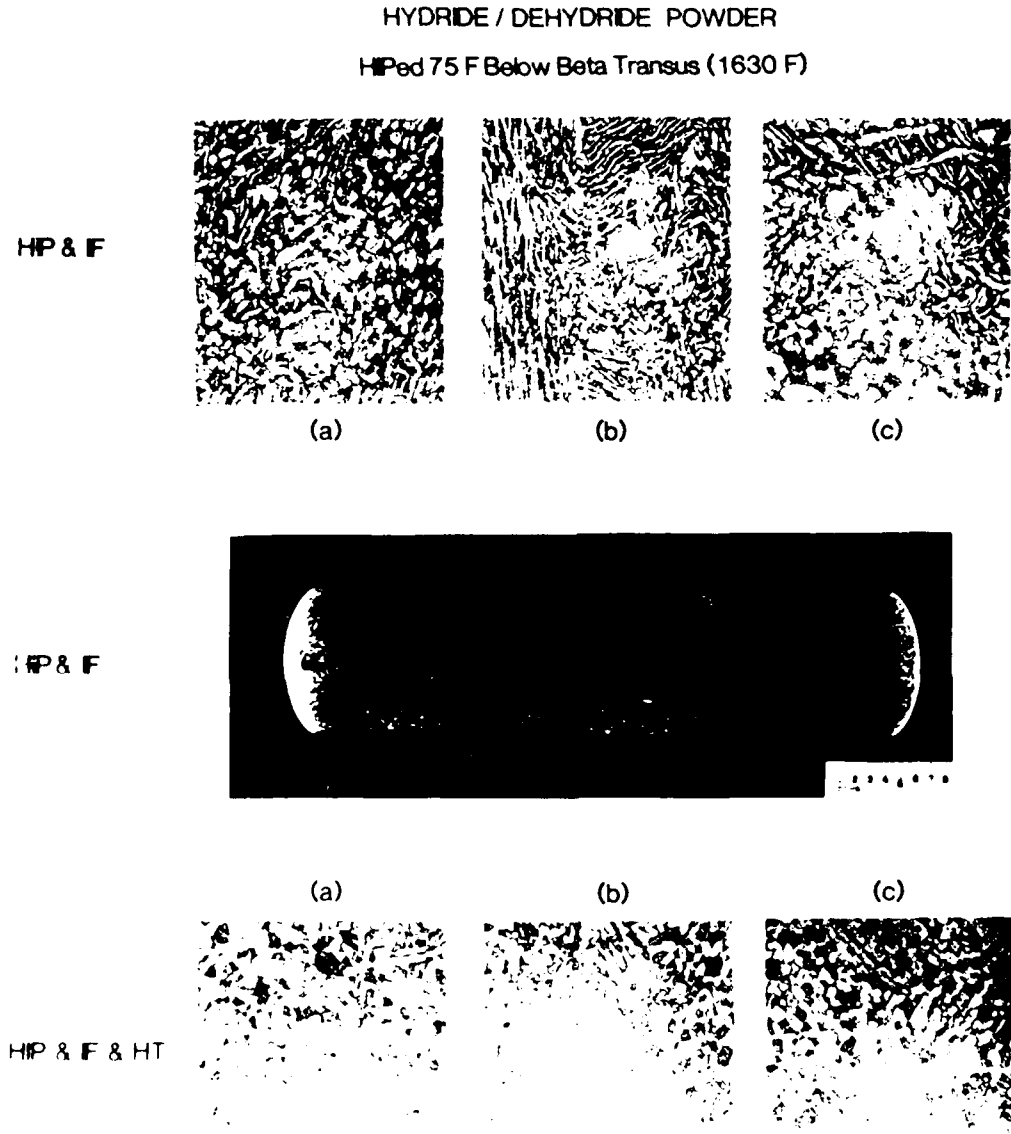


Figure 11.

phase is finer, deformed, and broken up. This is demonstrated for both the HIP + IF and HIP + IF + HT conditions in α + β HIP'd HDH powder in Figure 11.

a. Microstructure Development

The as-HIP'd microstructures of the HDH and REP powders are shown in Figures 7-10, for both sub-transus and supra-transus HIP'ing. The alpha phase tends to be of lower aspect ratio after sub-transus HIP'ing (23, 24, 25), with the alpha lathes arranged in a Widmanstatten structure. Supra-transus material contained predominately alpha colonies and a much larger amount of grain boundary alpha than in the sub-transus case.

In all cases isothermal forging to a 50% reduction caused a bending of the alpha plates towards a direction perpendicular to the forging direction (Figure 11, HIP & IF (23, 24, 25)).

Heat-treatment #1 (1650°F -1/2hr WQ+ 1050°F -1/2hr) produced different microstructures depending on whether the REP or HDH was involved. The 1650°F anneal reduced the amount of primary alpha to about 15% in the case of the REP (which had a beta transus of about 1705°F) but only to 45% in the case of the HDH (which because of the higher oxygen content had a beta transus of about 1750°F). There was also a large reduction, for both powder types, in the aspect ratio of the primary alpha depending on whether the prior HIP'ing had been above or below the transus. Supra-transus HIP'ing resulted in more elongated primary alpha while in both powder cases sub-transus HIP'ing resulted in more globular primary alpha after the sub-transus IF. The reason for this difference is probably because the strain produced during HIP'ing and IF is additive, this larger amount of strain in the alpha reduces its aspect ratio (23, 24, 25). The final age at 1050°F gave a final alpha precipitation (transformation) between the primary alpha regions which raises the strength level (26).

Heat-treatment #2 (1350°F -6hrAC+ 1680°F -3hr AC+ 1350°F -3hrAC) generally gave the same microstructural features in the four conditions (powders and HIP'ing conditions) as for heat-treatment #1. Sub-transus HIP'ing followed by IF and heat-treatment #2 gave more globular primary alpha than supra-transus HIP'ing. Again because of the beta transus difference the REP exhibited less

primary alpha than the HDH. The volume fraction of primary alpha is higher in this case because (a) AC followed the anneal (1680°F for condition #2, 1650°F for condition #1) and the aging treatment for condition #2 was 300°F higher (1350°F for condition #2, 1050°F for condition #1). It should be noted that in agreement with previous work (22) that the amount of grain boundary alpha was reduced by the triplex treatment. Because the "dead-zone" regions are subjected to less work (e.g., area (a) in Figure 11 compared to area (b) there is less globularization and more continuous grain boundary alpha in these regions.

Heat-treatment #3 (1450°F-2hr FC 1000°F AC) showed little tendency for globularization of the alpha phase since the annealing temperature is significantly below the beta transus (23, 24, 25).

b. Heat Treatment Selection For Phase II

The objective of heat treatment was to refine the α phase morphology and break up the continuous grain-boundary α leading to improved mechanical properties. Based on this phase of the work the STA and HT conditions were chosen over the AN condition for more detailed evaluation in Phase II. They are designated HT1 and HT2 respectively in Phase II. This selection was made based on the aspect-ratio of the alpha (low desirable) (26) and the amount of grain boundary alpha (minimum amount preferred (21)). For these reasons the β HIP'd process was eliminated from Phase II.

2. PHASE II - MECHANICAL PROPERTY STUDY

Two heat treatments selected from Phase I results were investigated in this part of the program. They were applied to as compacted billets before IF and again after IF as shown in Figure 1b. A total of 20 thermo-mechanical conditions were evaluated (Figures 1b and 2). Microstructures for those receiving HT1 are presented in Figure 12. Microstructures resulting from HT2 are in Figure 13.

Microstructure development and interpretation will be discussed in detail. Mechanical properties are then presented followed by fractographic results and a discussion tying them all together.

TI-6AL-6V-2SN COMPACTED POWDER MICROSTRUCTURES
(HEAT TREATMENT #1)

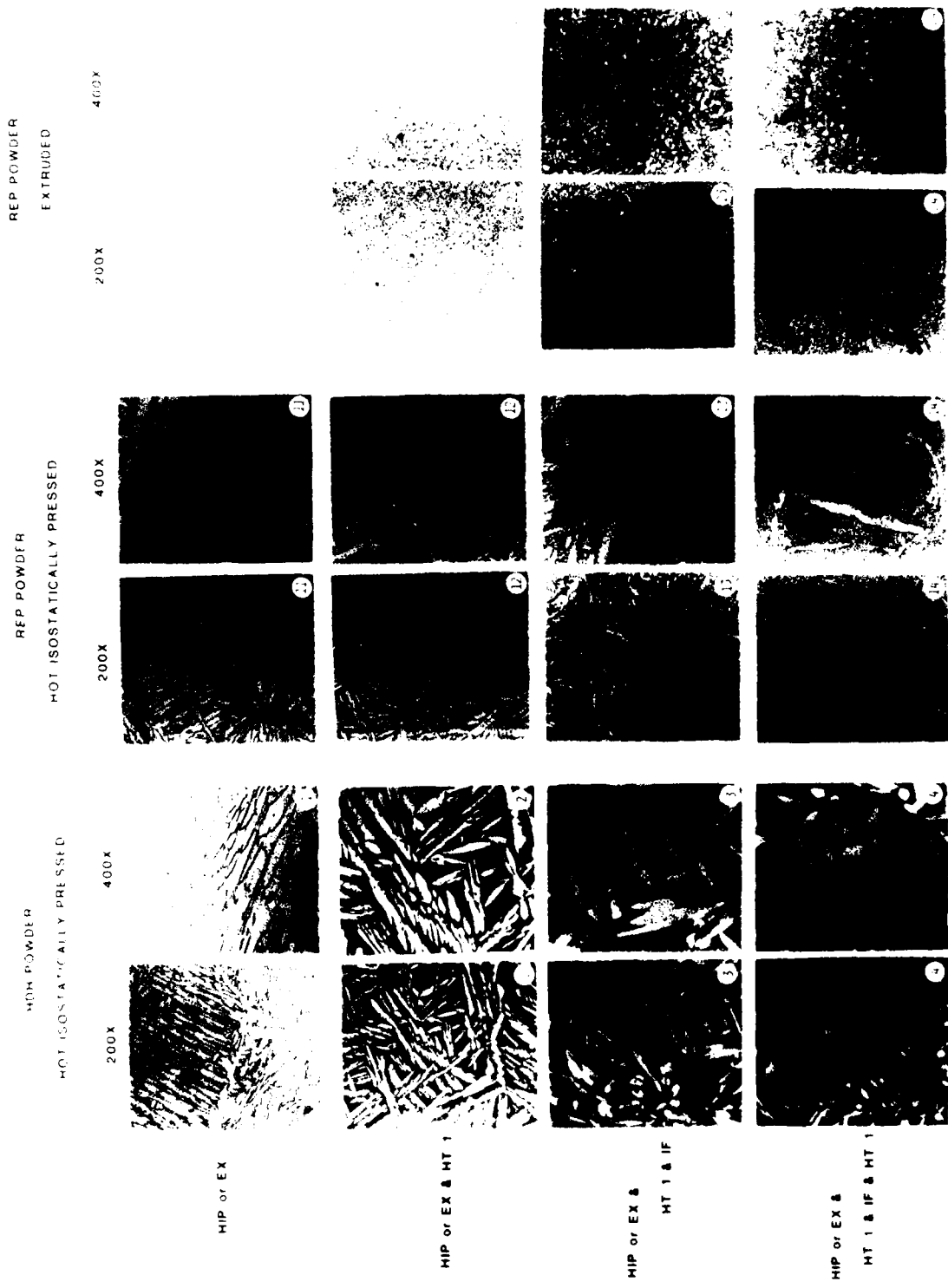
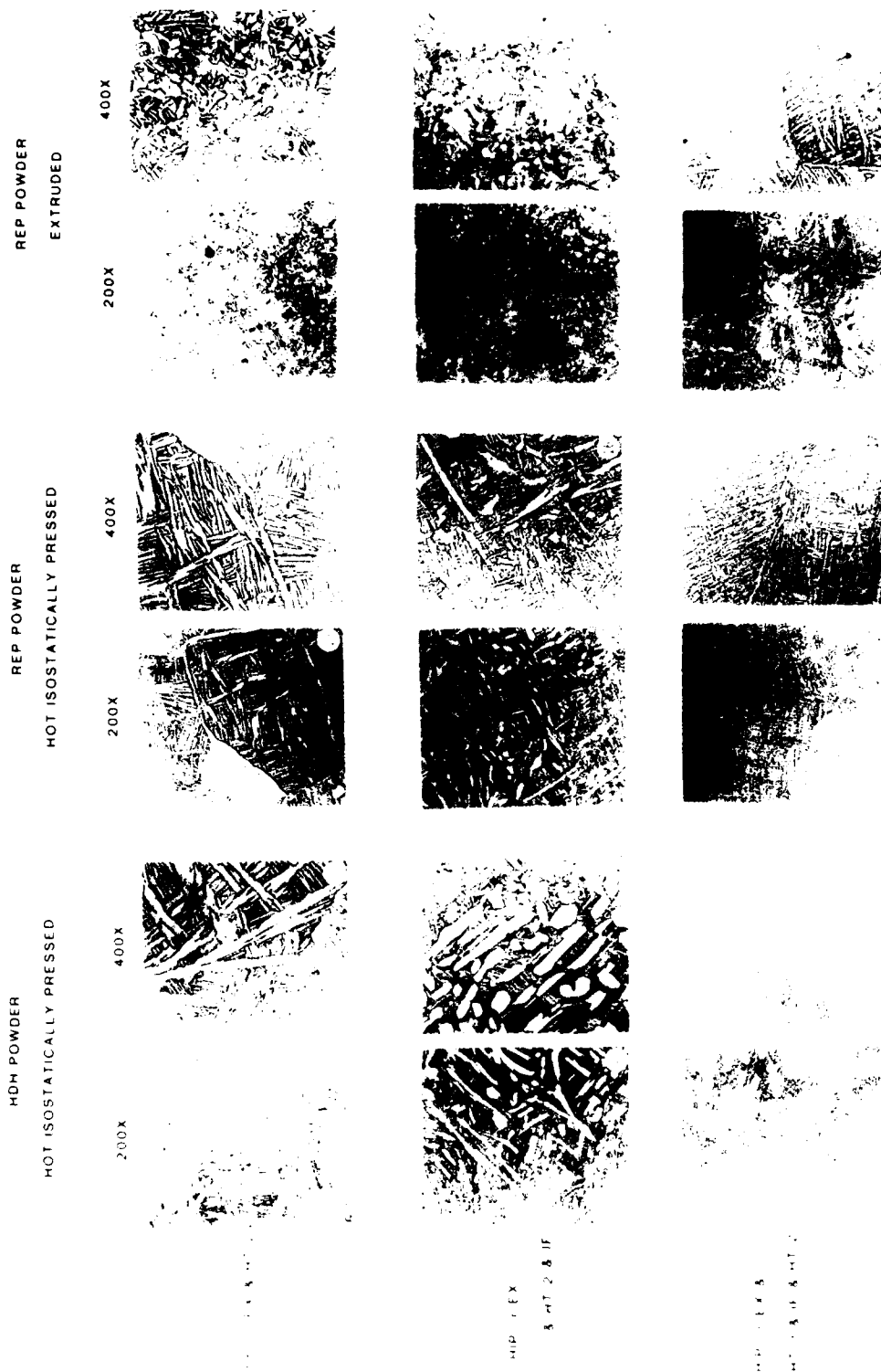


Figure 12

TI-6AL-6V-2SN COMPACTED POWDER MICROSTRUCTURES
(HEAT TREATMENT #2)



a. Microstructure Development

In this phase, twenty (20) microstructural conditions (Figure 1b) were studied and mechanically tested. Based on a preliminary observation of all twenty microstructure it was concluded that the beta transus temperatures of the two materials were:

HDH: $T_B = 1720^{\circ}\text{F}$

REP: $T_B = 1680^{\circ}\text{F}$

The higher beta transus temperature of the HDH powder material is due to the higher oxygen level. The four (4) thermal excursions used in developing the microstructures were:

HIP'ing at 1630°F

HT1 at 1650°F

HT2 at 1680°F

IF at 1650°F

To be able to interpret the microstructures, Table 4 shows how close each type of compact material was to the beta transus temperature at each of these thermal excursions.

Table 4: Proximity of Each Thermo-Mechanical Process Step to the Beta Transus Temperature ($^{\circ}\text{F}$)

Compact Material/Process	HIP	HT1	HT2	IF
HDH	-90	-70	-40	-70
REP	-50	-30	0	-30

The information in Table 4 is useful in understanding the ratio between primary and secondary alpha in these microstructures.

The following statements are also needed for a proper interpretation of the microstructures:

a. The microstructure of the as produced HDH powder is lenticular alpha in a colony arrangement within beta grain structure (27). This structure will be termed "an alpha colony structure."

b. The microstructure of as produced REP powder particles is martensitic (9).

c. A minimum of 80% $\alpha + \beta$ deformation is needed to fully transform lenticular primary alpha into a low aspect ratio morphology upon a subsequent recrystallization anneal (24). The 50% deformation IF was only sufficient to partially change this morphology.

d. The morphology of the secondary alpha is determined by the cooling rate from the maximum temperature and the subsequent aging treatment.

HT1: The 1650°F treatment followed by a water quench and a low temperature aging (1050°F) resulted in the finest secondary alpha in this work.

HT2: The 1680°F treatment followed by the air cool and high temperature aging resulted in a coarser secondary alpha structure.

IF: Judging from the microstructures of the as IF'd material, the cooling rate from the forge press was slow enough to develop a relatively coarse secondary alpha.

b. Microstructure Interpretation

Four thermo-mechanical process conditions are evaluated. They are shown for the HT1 microstructure in Fig. 12 and for the HT2 microstructure in Fig 13.

(1) As Compacted Structures

The as-HIP'd HDH powder (#1) is typical of an alpha colony structure which was exposed to long term heating high in the $\alpha + \beta$ phase field followed by a very slow cooling. These caused the lenticular alpha structure to substantially coarsen but still retained the general appearance of the alpha plate colonies. It is important to remember that this coarse lenticular alpha is the basic morphology of the primary alpha in most subsequent HDH conditions.

The as-HIP'd REP condition (#11) is typical of powder that was HIP compacted very close to the beta transus temperature (3). It consists of a high volume fraction of coarse, high aspect ratio alpha. Some of the alpha plates are arranged in a morphology which resembles the colony structure. However, it was not demonstrated yet that these alpha plates share the common orientation of alpha plates in a typical colony structure (28). This coarse alpha plate structure is the basis for most primary alpha morphologies in the subsequent REP condition which were treated below the beta transus temperature.

The as-extruded REP powder was not evaluated metallographically in the study. However from the HT1 condition (#22), it could be assumed that it had a predominantly low aspect ratio alpha morphology due to the alpha + beta work during extrusion. The equiaxed alpha morphology is evident in all sub transus heat treated conditions in contrast to the lenticular primary alpha morphology in the HIP'd condition treated below the beta transus temperature.

(2) Compacted + Heat Treated Structure

HDH: HT1 (#2) (Figure 12) resulted in a high volume fraction (approximately 70%) of coarse high aspect ratio primary alpha, the result of heat treating at 70°F below T_B , and a very fine secondary alpha which is typical of the type of heat treatment. HT2 (#5) (Figure 13) resulted in a smaller amount of primary alpha (approximately 50%) with coarser primary alpha which is typical of this heat treatment.

REP (HIP): HT1 (#12) (Figure 12) resulted in approximately 50 vol. pct. of lenticular primary alpha in a fine secondary alpha matrix. HT2 (#15) (Figure 13) was done right on the T_B (see Table 4) resulting in a typical beta annealed alpha colony structure.

REP (EXTRUSION): HT1 (#22) (Figure 12) resulted in a combination of 50 vol. pct. fine equiaxed primary alpha with medium coarseness secondary lenticular alpha. HT2 (#25) (Figure 13) resulted also in a 50 vol. pct. mixture of coarser equiaxed primary alpha and coarser lenticular secondary alpha.

(3) Isothermally Forged Structures

HDH (#3 and #6): Both HT1 and HT2 show evidence of partial breaking up of the coarse primary alpha lamellae into long aspect ratio alpha. The coarse secondary lenticular alpha is the result of the slow cooling rate from the forge press. There is about 50 vol. pct. primary alpha present.

REP (HIP) (#13 and #16): Both HT1 and HT2 show 50 and 40 vol. pct. (respectively) of partially recrystallized primary alpha in a coarse lenticular secondary alpha matrix.

REP (EXTRUSION) (#23 and #26): Both HT1 and HT2 show 40 and 20 vol. pct. (respectively) of globular primary alpha in a matrix of lenticular secondary alpha.

(4) IF + Heat Treated Structure

HDH (#4 and #7): These microstructures resemble conditions #2 and #5 (respectively), since they were subject to the same heat treatment. However, in the latter condition the primary alpha is partially globularized (the result of the IF) and for an unknown reason, there is less primary alpha (approximately 30 vol. pct.).

REP (HIP), HT1 (#14), The microstructure is now predominately fine secondary alpha, the result of heat treating close to the T_B (Table 4) with only 20 vol. pct. primary lenticular alpha. It is not understood why the primary alpha has such a high aspect ratio following the IF + HT1. HT2 (#17) is a beta annealed alpha colony structure resulting from treating the material at the beta transus temperature. It shows a typical alpha plate arrangement within a prior beta grain structure. Grain boundary alpha along the prior beta grain boundaries can also be seen.

REP (EXTRUSION), HT1 (#24) is similar to #14 but all the primary alpha is globularized and more finely dispersed. HT2 (#27) is also a beta annealed structure, as is #17, showing alpha plate colonies, and prior beta grains.

c. Mechanical Properties

As described in Section III-2-f, Mechanical Testing, tensile and fracture toughness tests were performed on each of the 20 samples described in Figure 1b. Blanks used to machine the 0.252 in. guage diameter tensile and precracked Charp V-notch samples are shown in Figure 2. Results from the tests are given in Table 5.

Ductility and toughness is plotted as a function of yield strength in Figures 14-18 and as a function of ultimate tensile strength in Figures 19-23. The as HIPed + IF properties reported in Ref. 1 for both HDH and REP powder compacts are shown in black symbols on each curve. These are the reference points to compare the results of both heat treatments. The RA result for REP powder is out of line with all other results. Consequently, ductility comparisons will be made from elongation results only for REP powder conditions. High and low boundary extremes are drawn on each plot.

(1) Heat Treatment 1

In all cases the strength level is markedly increased by HT1 while ductility is lowered. Fracture toughness as measured by K_Q increases slightly while K_V (W/A) decreases slightly for both HDH and REP powder.

The main effect of HT1, then, is to increase strength roughly 25ksi while more than halving ductility and holding a comparable fracture toughness compared to the un-heat treated HIP + IF material.

(2) Heat Treatment 2

The HT2 effect on mechanical properties is not quite as consistent. In all cases the strength level remains the same. For HDH powder material, ductility increases significantly with some indication of a modest increase in fracture toughness [K_Q increases and K_V (W/A) remains at the same level]. For REP powder, there is a small decrease in ductility with a substantial increase in fracture toughness. Since the REP powder is the preferred production procedure due to higher purity and reliability, it will be used to critique HT2.

Results show then that HT2 increases fracture toughness 50% to 100% while maintaining the same strength level and close to the same ductility (15% vs 20%) of the un-heat treated HIP + IF material.

Clearly there is a big difference in the effect of HT1 and HT2 on mechanical properties. This is expected from the different peak temperature and even more from the very different final annealing temperature. These different treatments produce very different microstructures and, therefore, different properties. This is discussed further in Section IV-2-e, Correlation of Microstructure, Mechanical Properties and Fractography.

The objective of this program was to find a way to increase toughness and/or ductility without losing strength. HT2 was found to be a successful way to do that.

TABLE 5
Ti-6Al-6V-2Sn COMPACTED POWDER SAMPLE THERMO-MECHANICAL TREATMENT AND MECHANICAL PROPERTIES

Sample	Powder	Billet Condition	Isothermal Force Peak Load (Tons)	σ_y (ksi)	c_u (ksi)	Elong. (%)	R/A	K_Q^{**} (ksi-in $^{1/2}$)	WA	K_V^{***} (ksi-in $^{1/2}$)
1	HDX	HIP	--	128	139	13	62	308	53	39
-	"	HIP+IF*	--	145	148	6	9	164	29	29
2	"	HIP+HT #1	--	159	168	2	38	94	34	34
3	"	HIP+HT #1+IF	53	149	155	13	17	46	126	19
4	"	HIP+HT #1+IF+HT #1	56	174	176	1	26	38	294	52
5	"	HIP+HT #2	--	133	140	12	4	52	130	34
6	"	HIP+HT #2+IF	48	139	151	13	14	46	168	39
7	"	HIP+HT #2+IF+HT #2	47	137	145	12	12	51	168	39
41	REP	HIP	--	118	129	18	21	44	202	43
-	"	HIP+IF*	--	135	138	20	45	32	340	56
12	"	HIP+HT #1	--	145	155	12	16	42	164	39
13	"	HIP+HT #1+IF	45	130	142	14	23	54	392	60
14	"	HIP+HT #1+IF+HT #1	43	164	172	6	2	38	69	25
15	"	HIP+HT #2	--	126	136	18	22	40	611	74
16	"	HIP+HT #2+IF	42	128	140	16	22	70	396	60
17	"	HIP+HT #2+IF+HT #2	42	122	136	15	17	68	477	66
21)	REP	Extruded (not evaluated)	--	--	--	--	--	--	--	--
22	"	Ex+HT #1	--	158	160	11	12	43	84	28
23	"	Ex+HT #1+IF	41	136	143	10	10	56	239	47
24	"	Ex+HT #1+IF+HT #1	42	165	170	6	9	34	52	22
25	"	Ex+HT #2	--	127	135	14	16	40	264	49
26	"	Ex+HT #2+IF	39	135	143	15	26	46	252	48
27	"	Ex+HT #2+IF+HT #2	38	123	135	15	20	50	594	73

HIP : 1630°F 2hr 15ksi by Argon - If...1650°F 0.3 ipm Polygraph Lubricant/AC
 HT#1: 1650°F 1/2hr/WQ/1050°F 24hr/AC - HT#2: 1350°F 6hr/AC/1680°F 3hr/AC/1350°F 3hr/AC

*Ref 20

** Slow bend pre-crack Charpy measurements

$$\text{A, } K_V^2 = \left(\frac{W}{A} \right) \cdot \left[\frac{E}{2(1-\nu^2)} \right]$$

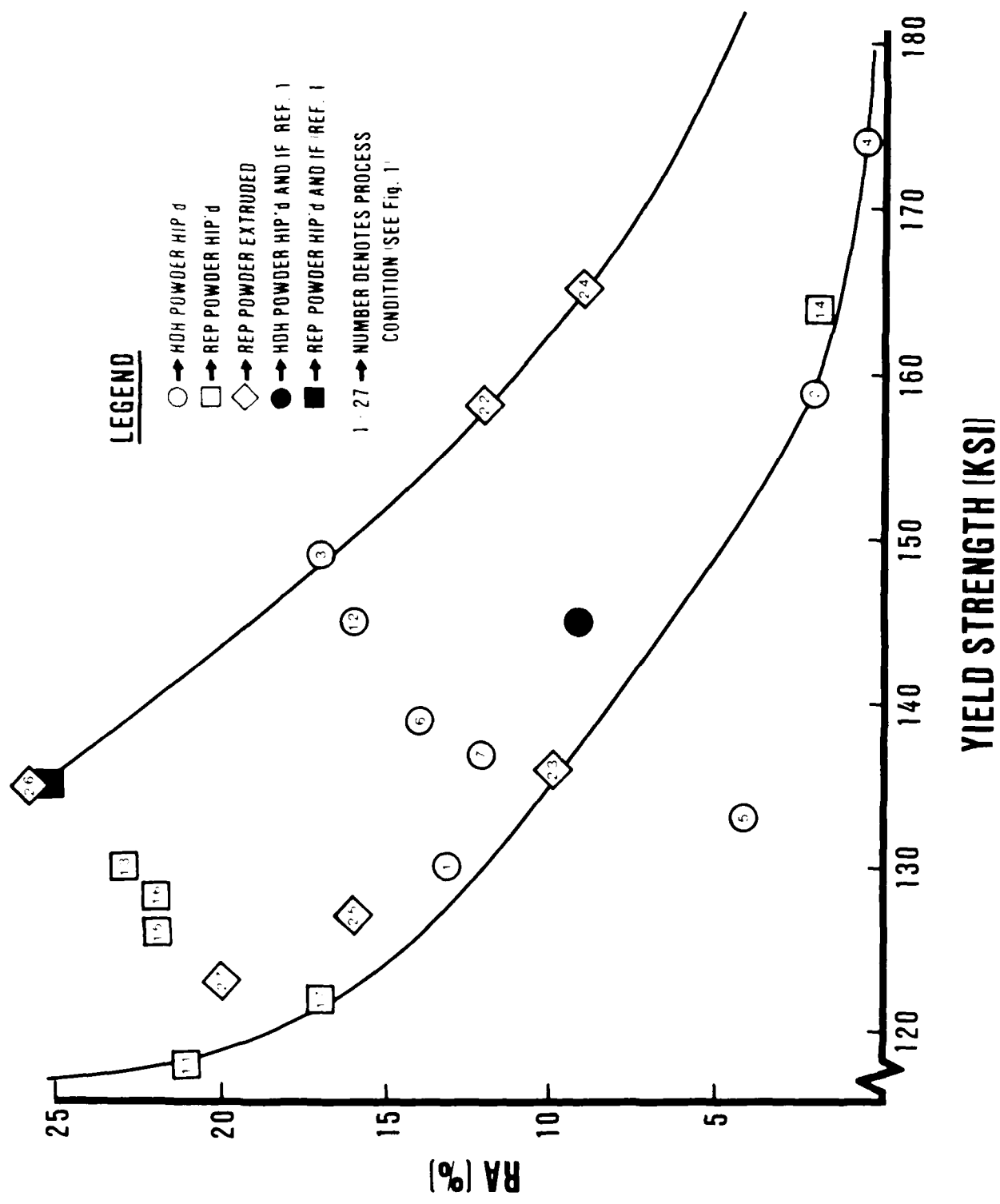


Figure 14. Ductility as measured by RA is a function of Y.S. for 20 conditions as detailed in Figure 1b.

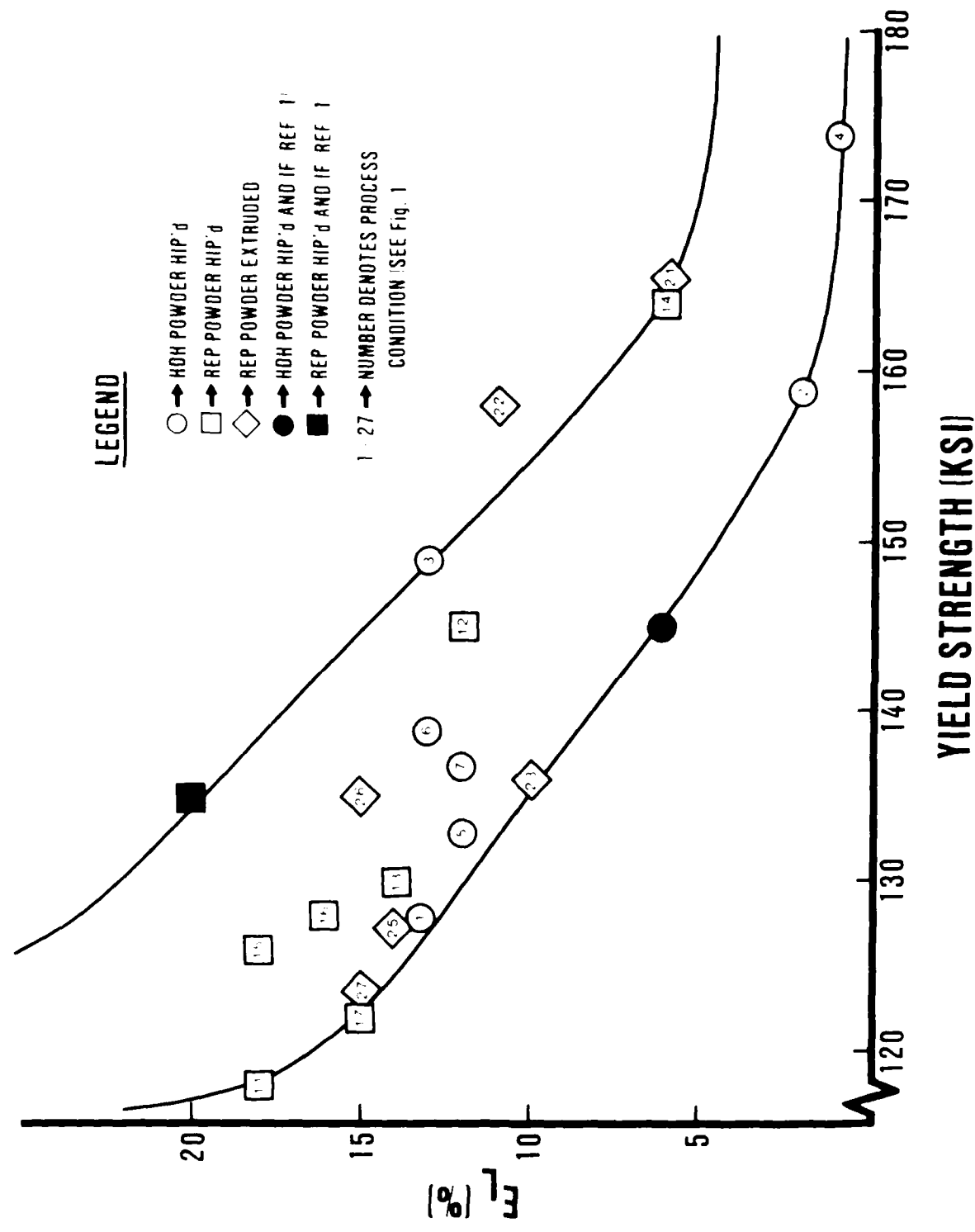


Figure 15. Ductility as measured by elongation as a function of Y.S. for 20 conditions detailed in Figure 1b.

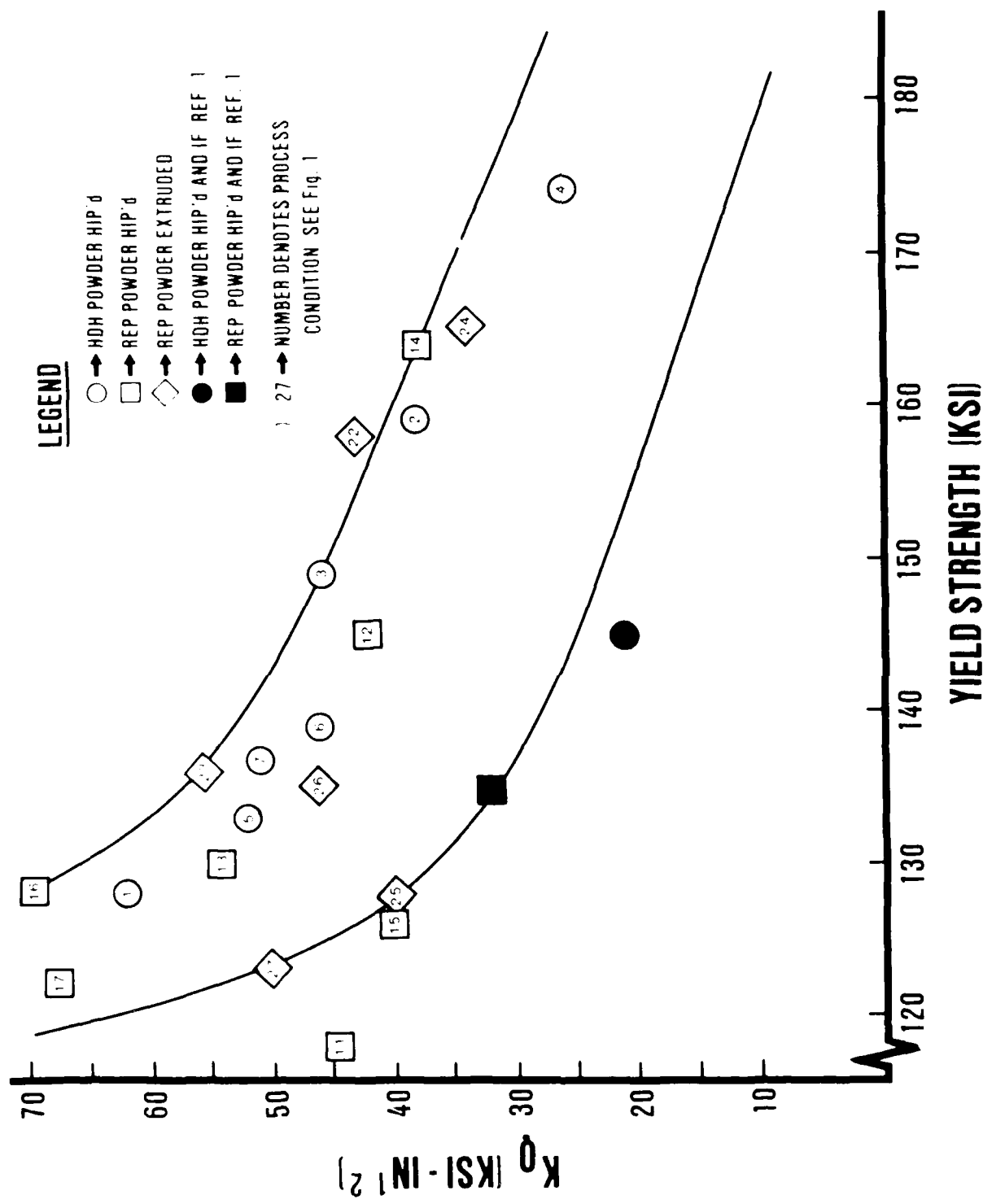


Figure 16. Fracture toughness as measured by K_Ic as a function of Y.S. for 20 conditions detailed in Figure 1b.

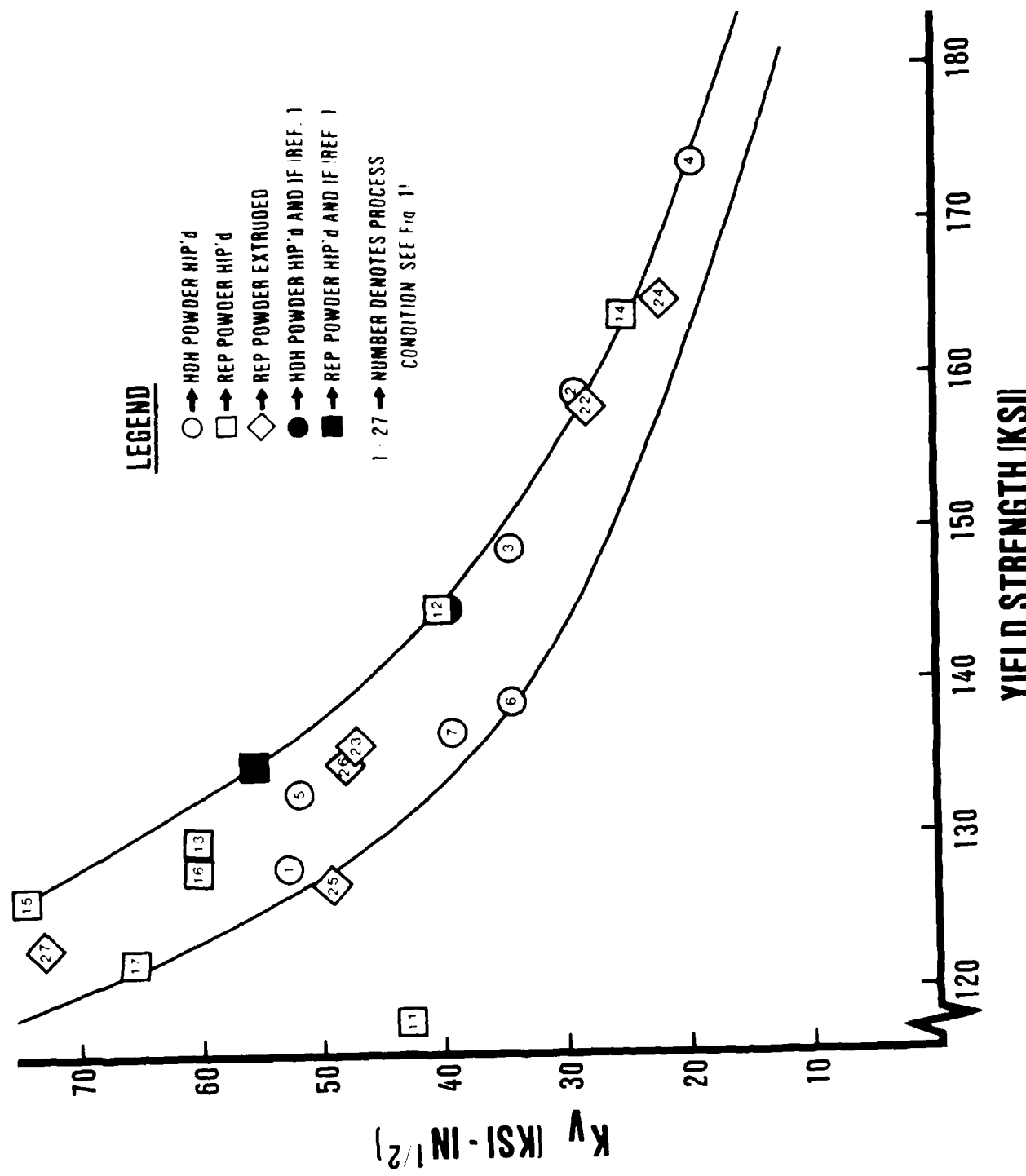


Figure 17. Fracture toughness as measured by K_V (calculated from W/A) as a function of Y.S. for 20 conditions detailed in Figure 1b.

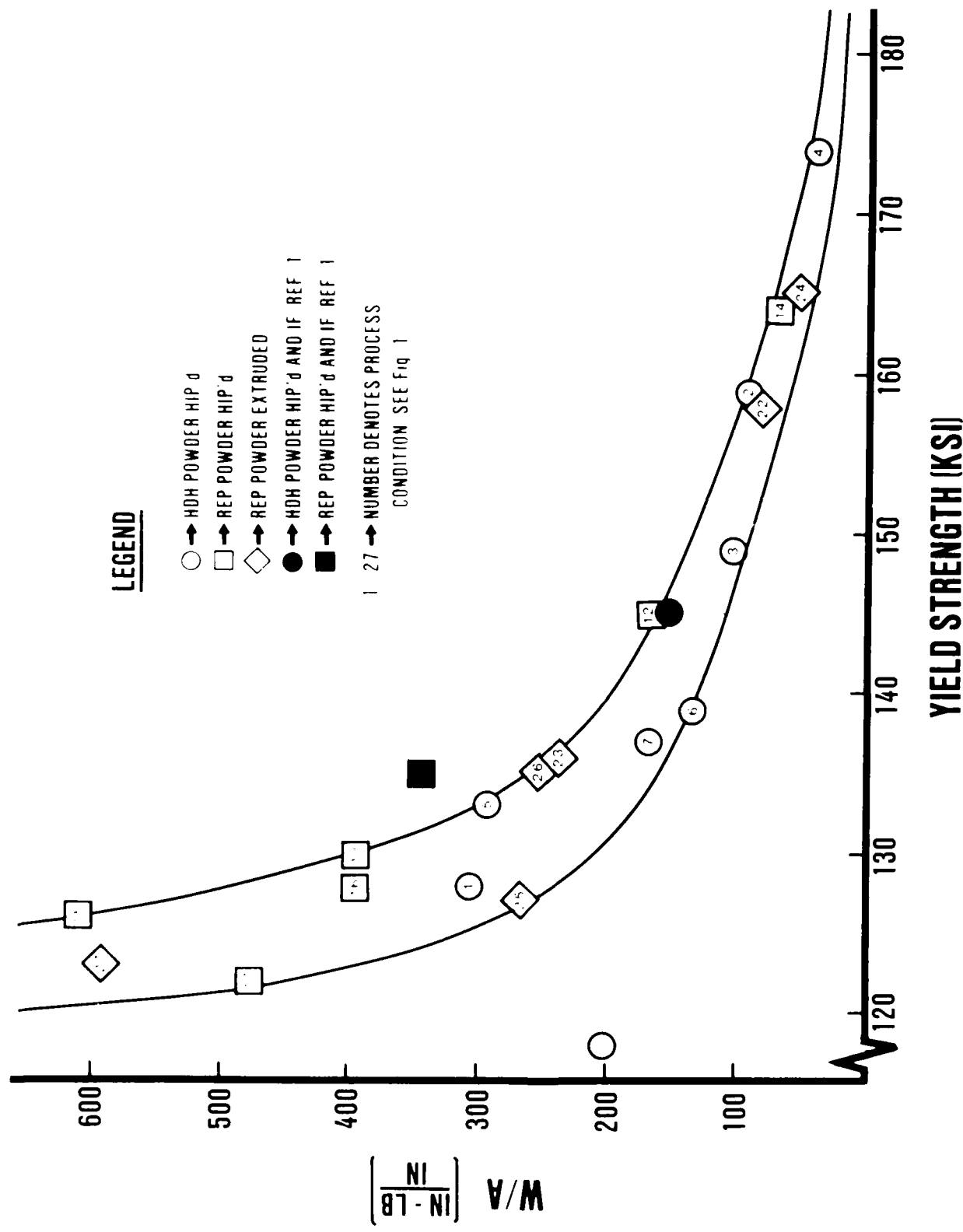


Figure 18. Fracture toughness as measured by W/A as a function of Y.S. for 20 conditions detailed in Figure 1b.

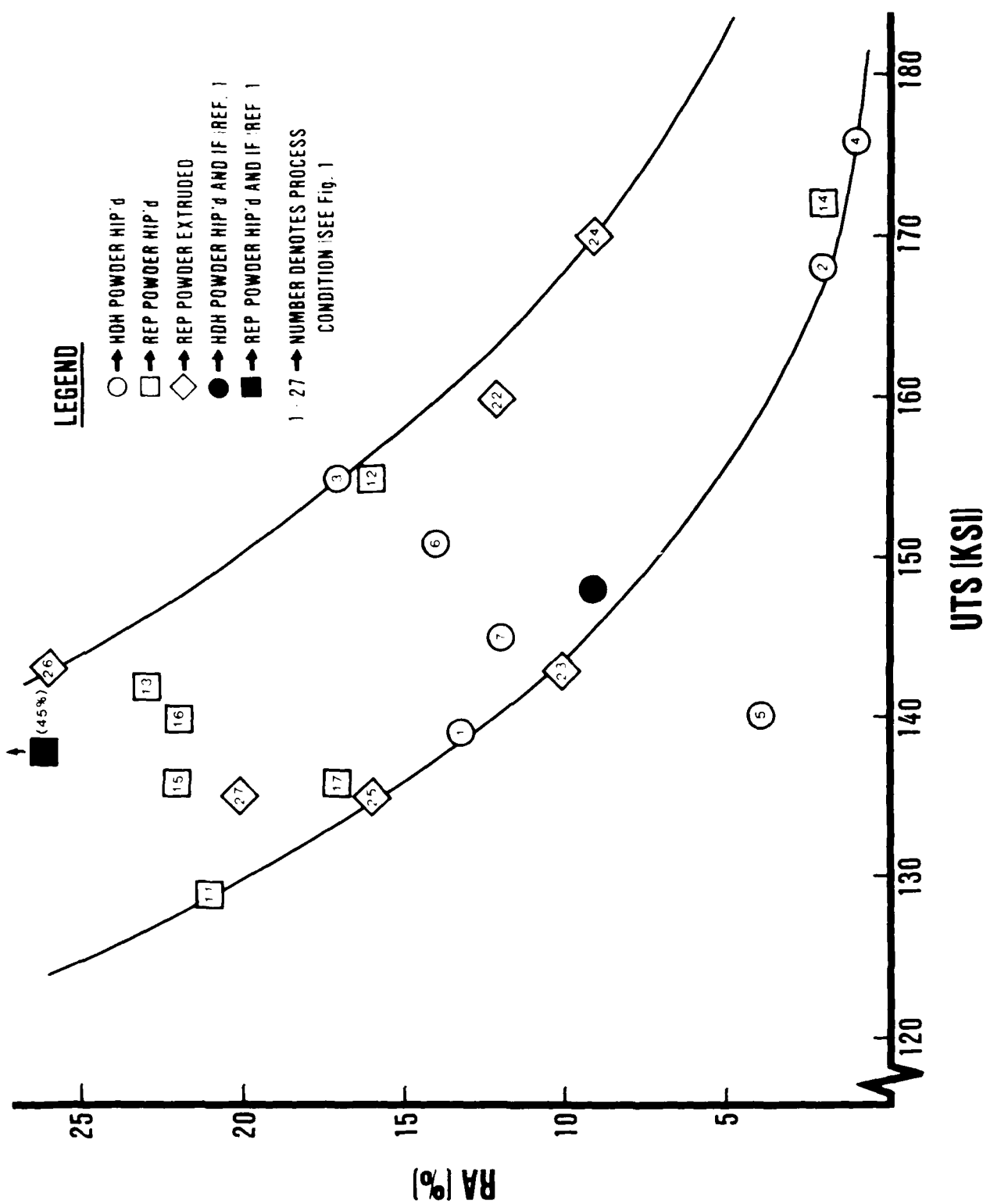


Figure 19. Ductility as measured by RA as a function of UTS for 20 conditions as detailed in Figure 1b.

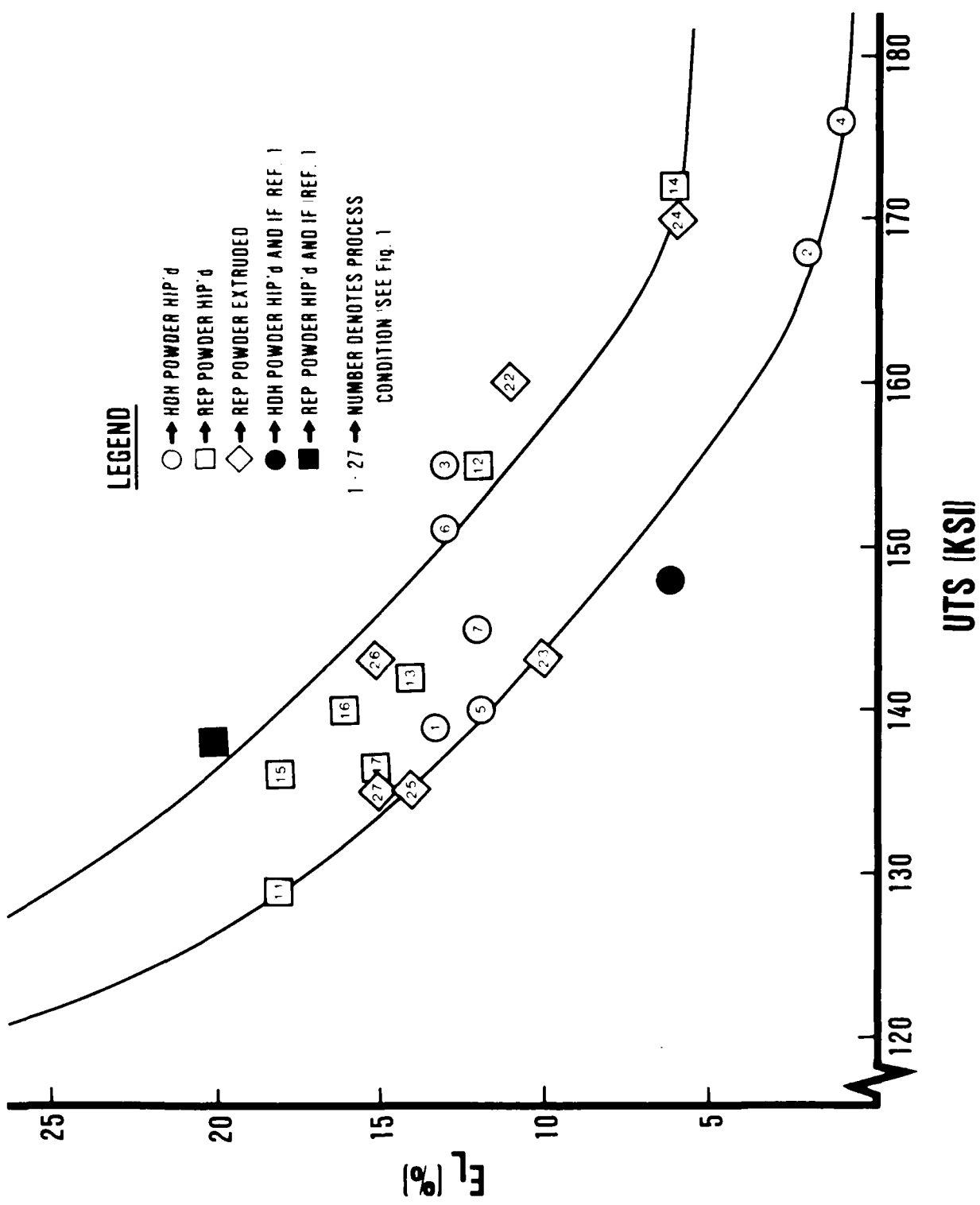


Figure 26. Ductility as measured by elongation as a function of UTS for 20 conditions detailed in Figure 1b.

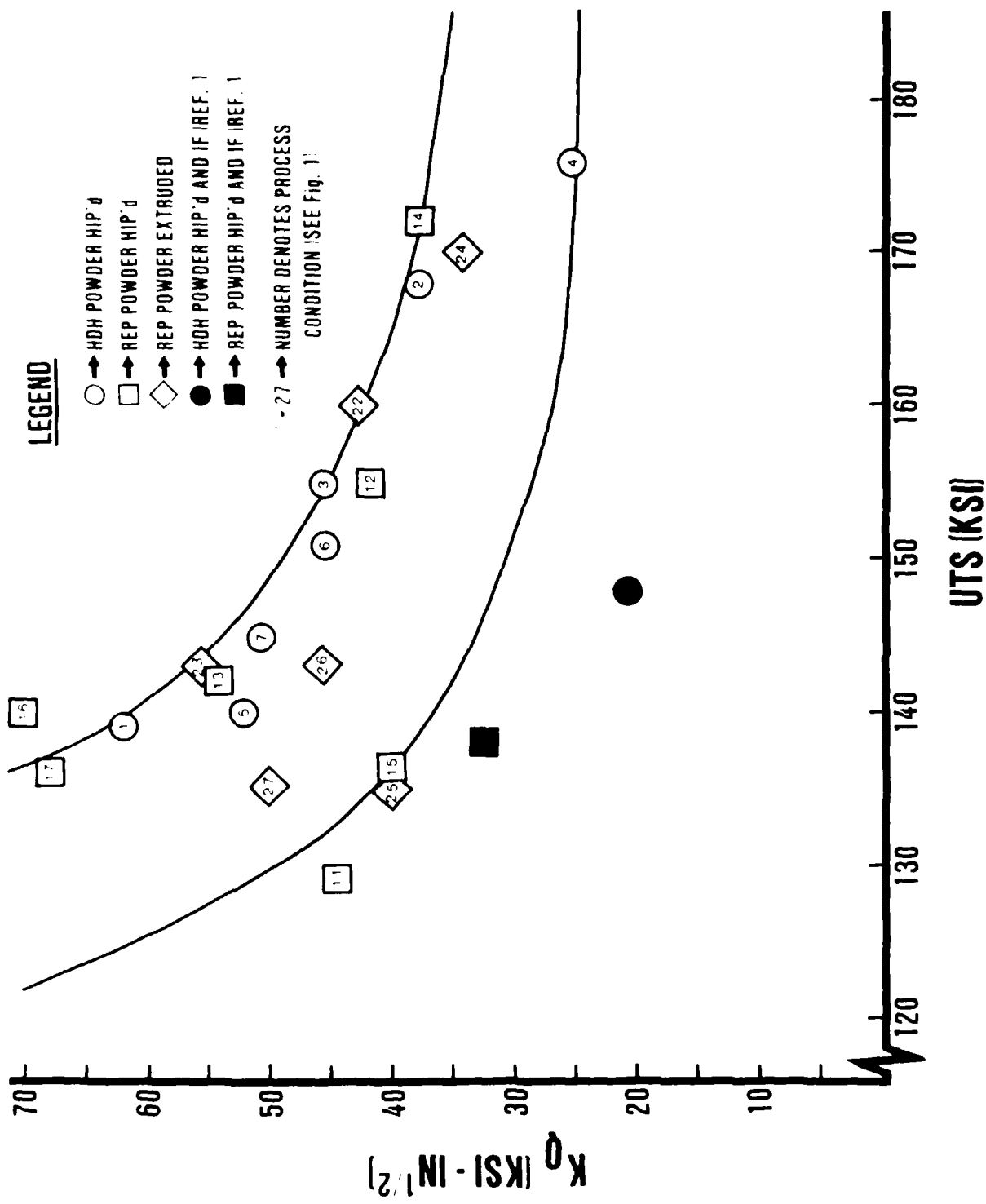


Figure 21. Fracture toughness as measured by K_Ic as a function of UTS for 20 conditions detailed in Figure 1b.

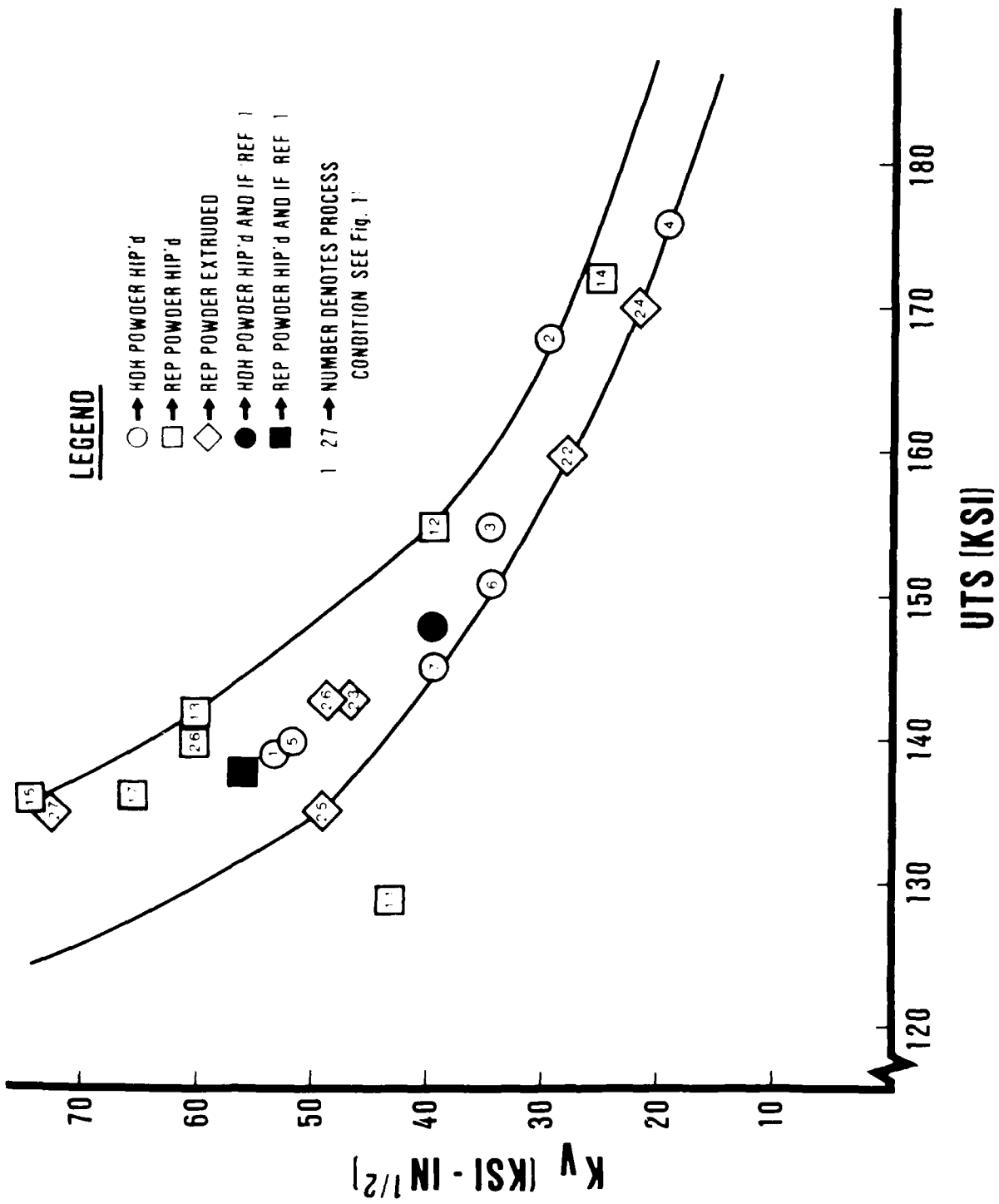


Figure 22. Fracture toughness as measured by K_V (calculated from G/A) as a function of UTS for 20 conditions detailed in Figure 1b.

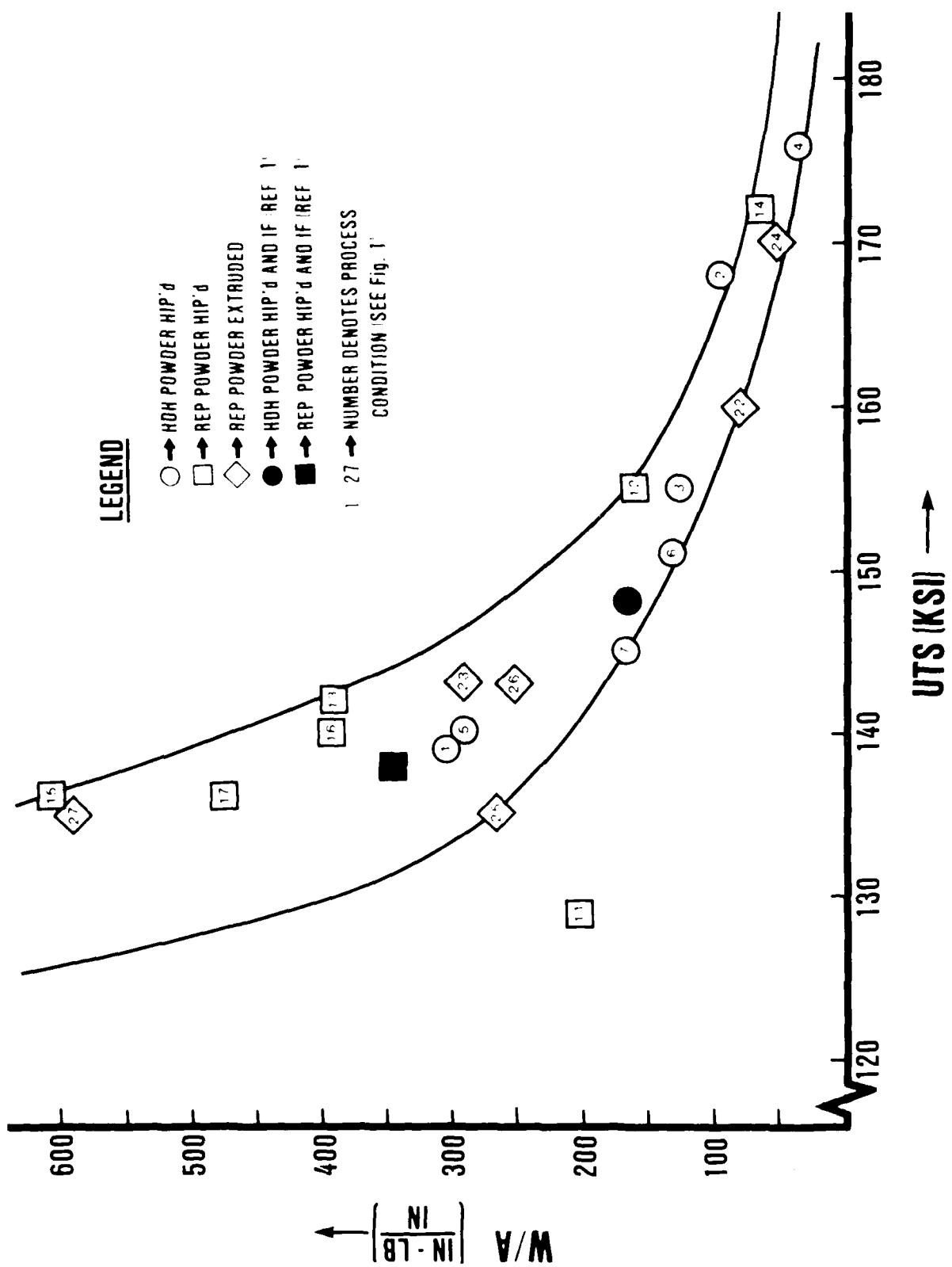


Figure 23. Fracture toughness as measured by W/A as a function of UTS for 20 conditions detailed in Figure 1b.

d. Fractography

Scanning electron micrographs of both tensile and charpy fracture surfaces are shown in Figures 24-26 for six conditions. Samples #4 and #7 are arranged together in Figure 24 and #24 and #27 are together in Figure 25 to compare HT1 and HT2 for the same powder and compaction conditions. The other two conditions examined, #3 and #22, are in Figure 26.

Each condition is discussed individually below.

(1) Sample 27

This condition is the easiest to analyze from fractographic point of view and also to correlate the microstructure to properties. Since the material has been above the beta transus temperature (T_p) it has a set of properties similar to P annealed or cast alloy conditions (namely low strength and high fracture toughness). The high fracture toughness is evident in the SEM fractographs, Figure 25, showing a tortuous crack path associated with both faceted fracture features and ductile dimpled zones. Similar fracture behavior was previously observed in titanium alloys treated to a similar condition which resulted in high fracture toughness values (29).

The relatively high tensile ductility of this condition sample is evident by the dimpled fracture surface visible on the tensile SEM fractograph, Figure 25. However, this is very uncommon because beta processed structure typically displays faceted tensile fracture associated with low tensile elongation.

(2) Sample 3

Condition number 3 has an excellent combination of tensile strength, ductility and fracture toughness. The good fracture toughness values are possibly the result of the coarse remnant primary alpha which lead to a tortuous crack path, and the relatively coarse secondary alpha (due to slow cooling following IF) which is also contributes to an improved fracture toughness when compared to the fine secondary alpha structure of the other

conditions. The fractographs show a good combination of faceted fracture features and ductile dimpled fracture regions. The high strength level can be interpreted on the basis of the relatively high volume fracture of the secondary alpha phase. The high tensile elongation is evident in the highly dimpled SEM fractograph of the tensile test specimen, Figure 26, and is probably associated with the deformation of the relatively coarse secondary alpha.

(3) Sample 22

This material condition is unique in this work since it has the highest volume fraction of equiaxed primary alpha. This microstructure condition is typically associated with good tensile strength and elongation but lower fracture toughness. The tensile SEM fractograph, Figure 26, shows a very fine dimple structure (on the order of 5μ) which corresponds to the grain size of the equiaxed primary alpha. This type of fracture is an indication of good tensile ductility. A very similar dimpled surface is evident on the fractographs of the fracture toughness specimens. This type of fine dimpled fracture is usually associated with a much less tortuous crack path leading to relatively low fracture toughness values (30).

(4) Sample 24

This sample condition has a much lower volume fraction of equiaxed alpha compared to condition #22 and a very high volume fraction of fine lenticular transformed beta. This is a typical duplex microstructure which is used extensively in gas turbine engine components when a good combination of properties is required. Similar to condition #22, it also displays very fine dimpled fracture features in both the fracture toughness and the tensile SEM fractographs, Figure 25. Comparison of the mechanical properties indeed shows that these two microstructural conditions are similar in their behavior.

In spite of the fact that this condition had almost the same processing route as condition #27 (the only difference is HT1 vs HT2), the beta solution treatment in condition #27 completely changed the microstructure, the fracture morphologies (Figure 25), and the subsequent set of mechanical properties (Table 5).

(5) Sample 4

Condition #4 microstructure is typified by a high volume fraction of very fine secondary alpha which resulted in the highest tensile strength obtained in this work but also the lowest tensile ductility and fracture toughness. This loss of ductility and toughness is common in titanium alloys processed and treated to maximum strength conditions. The tensile fracture surface (Figure 24) indicates several regions of very flat fracture features, possibly associated with regions of high aspect ratio primary alpha. These low energy fracture zones are, possibly, responsible for the tensile failure at early stages of deformation before a void formation mechanism, which typically leads to ductile dimple fracture, had the opportunity to develop.

The low value of the fracture toughness can not be explained on the basis of the fracture appearance, Figure 24. However, very low elongation and RA conditions, of the order of 1 to 2%, are almost always associated with very low fracture toughness values in titanium alloys.

(6) Sample 7

Condition #7 should be compared to condition #4 because it has the same processing route except for the use of HT2, instead of HT1, which resulted in the coarsest secondary lenticular alpha structure in this program. On the other hand, condition #4 displayed the finest secondary alpha obtained in the work. As a result, condition #7 has lower strength level than #4, high ductility and higher fracture toughness. The faceted fracture features on the tensile specimens (Figure 24) are typical of a fine alpha plate colony structure, and the alpha plate morphology can be easily resolved on these faceted fracture features.

The fracture toughness failure surface is similar in appearance to the fracture features observed in condition #27 which also has a fine alpha plate colony structure. Both samples received HT2 and Condition #7 and are expected to have nearly the same values of fracture toughness as Condition #27.

TI-6AL-6V-2SN TENSILE AND CHARPY V-NOTCH FRACTOGRAPH
HDH POWDER

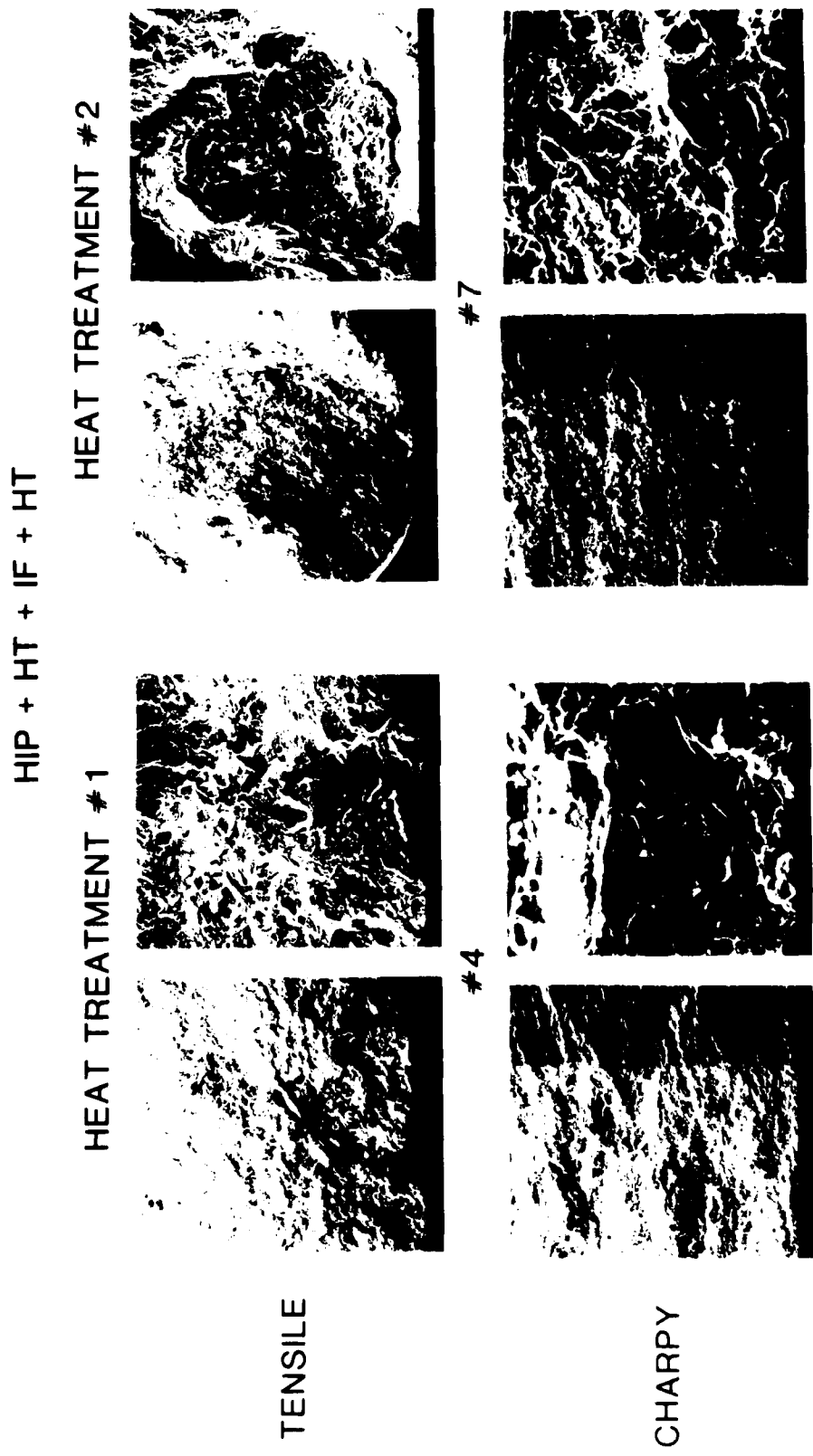


Figure 24. Scanning Electron micrographs comparing tensile and charpy specimen fracture surfaces of Llivirite Dehydride Powder material for both HT1 and HT2.

TI-6AL-6V-2SN TENSILE AND CHARPY V-NOTCH FRACTOGRAPHS
REP POWDER

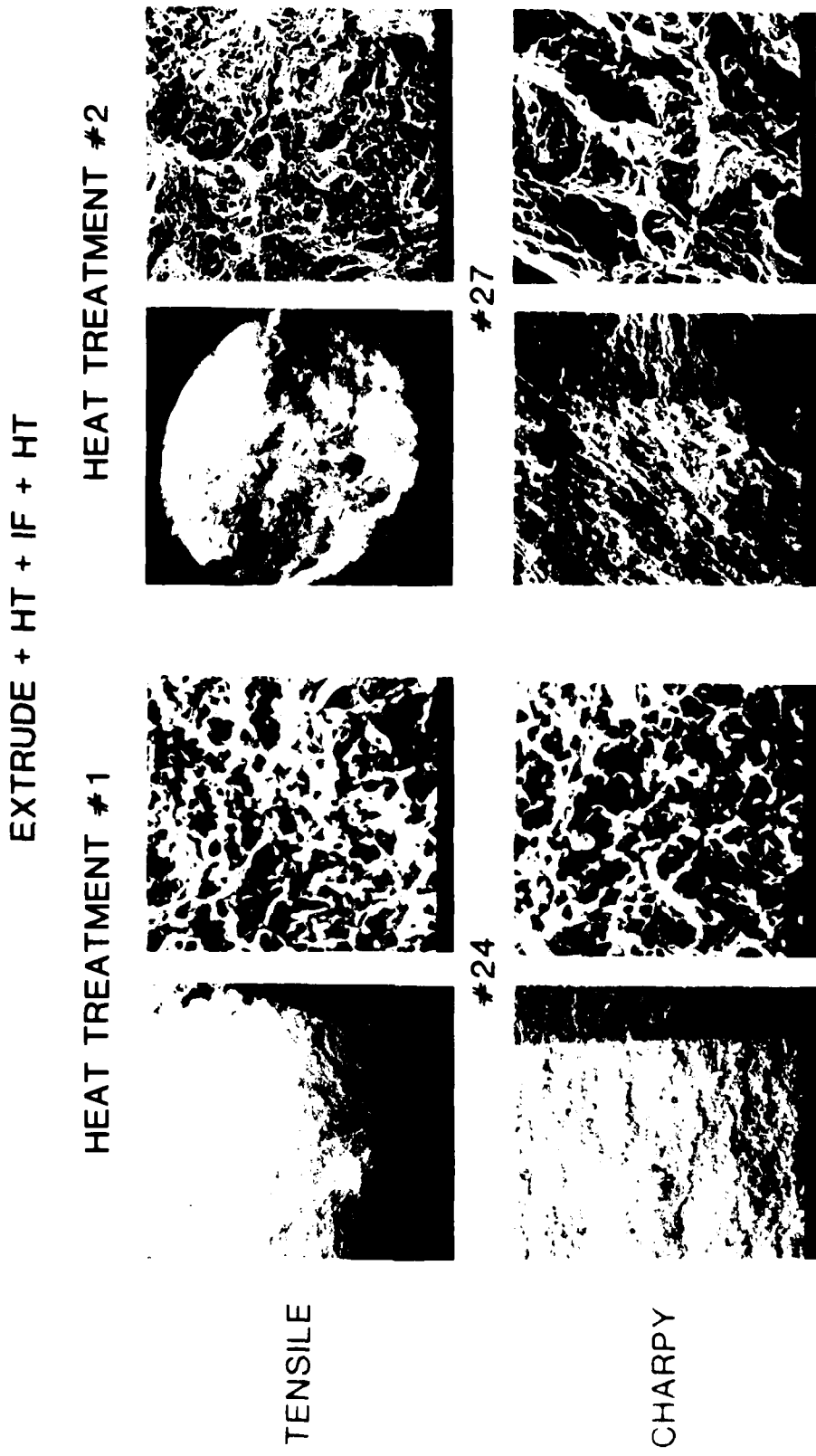


Figure 25. Scanning electron micrographs of Rotating Electrode Process Powder material comparing tensile and charpy specimen fracture surfaces for both HT1 and HT2.

TI-6AL-6V-2SN TENSILE AND CHARPY V-NOTCH FRACTOGRAPH
REP POWDER

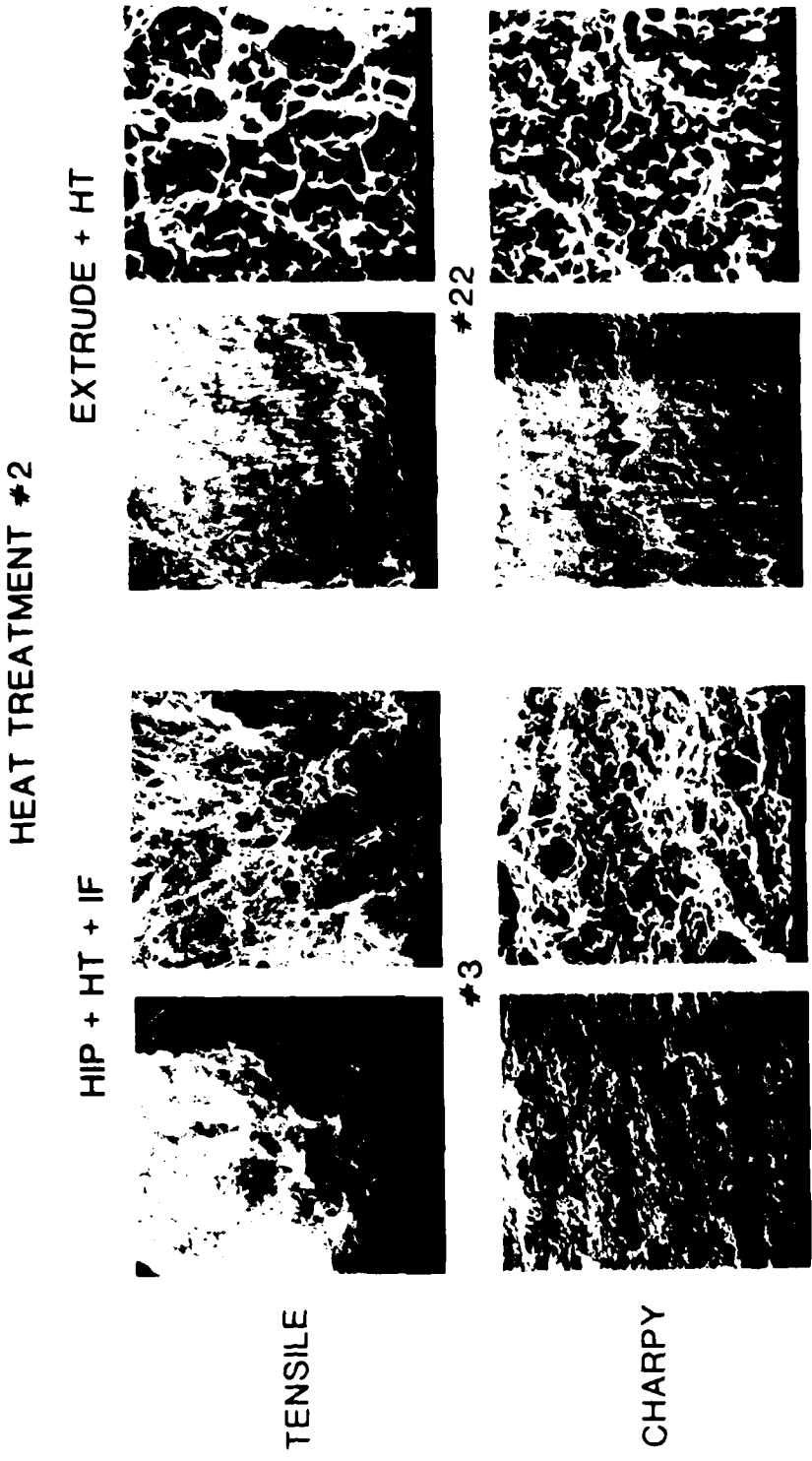


Figure 6. Scanning electron micrographs showing fracture morphology for a material condition (microstructure) exhibiting an excellent combination of tensile strength, ductility and fracture toughness (Sample #2), and for a sample with an unusually large equiaxed alpha grain microstructure leading to a dimpled fracture appearance typically resulting in high ductility and low fracture toughness.

e. Correlation of Microstructure, Mechanical Properties and Fractography

Microstructures have been grouped in Table 6 into categories to help correlate them with thermo-mechanical treatment and mechanical properties as described in Figure 1b and Table 2, respectively.

TABLE 6
MICROSTRUCTURE CLASS DESIGNATIONS WITH SAMPLE NUMBER AND UTS (KSI)

Microstructure Description	Sample Number (UTS - KSI)		
	HDH	REP-HIP	REP-EX
<u>Lenticular</u>			
Coarse	1 (139)	11 (129)	
Med.	5 (140)		
Fine		12 (155)	
<u>Equiaxed</u>			
Coarse			25 (135)
Med.			23 (143) 26 (UTS)
Fine			22 (160)
<u>Lenticular-Equiaxed</u>			
Coarse	7 (145)		
Med.	6 (151)	13 (142) 16 (140)	
Fine	3 (155)		
<u>Transformed Beta</u>			
Coarse		15 (136) 17 (136)	27 (135)
Fine	2(168) 4(176)	14 (172)	24 (170)

A number of consistent observations are possible from Table 6. Within each class of microstructure, strength level decreases as the structure coarsens. Also note that the HDH material is consistently stronger for the same microstructure, probably due to the higher oxygen content of this material.

TABLE 7: Microstructure Classification of the Tested Conditions

Designation	Condition No.	Primary Alpha		Secondary Alpha (Lenticular		Beta Annealed Structure	
		Lenticular		Equiaxed		Coarse (Colony)	
		Coarse	Fine	Coarse	Fine	Coarse	Fine (Widmansstatten)
BC	15,17,27						
BF	14						+
PLC	1,11	+					
PLC + SF	2,12	+					
PLC + SC	3,5,13	+					
PLF + SC	16		+			+	
PEF	21,23						
PEC	25						
PEF + SF	24					+	
PEF + SC	26					+	
PEC + SC	6,7					+	
PEC + SF	4					+	

The widest variation of properties within a microstructure group is between fine and coarse lenticular transformed β . Fine transformed β structures (2,4,14,24) produced by the low temperature [1050°F (566°C)] anneal of HT1 have markedly higher strength and lower toughness and RA, although the elongation is comparable to a number of other structures.

(1) Microstructure

The development of the microstructure was already discussed in detail in section IV-2-a of this report. Due to the fact that some conditions were treated at or near the beta transus temperature, a wide range of microstructural characteristics was obtained in the work which give an excellant opportunity to study the relationship of properties to a large variety of microstructures.

The two basic microstructures are lenticular alpha and low aspect ratio alpha. The development of these types was already discussed in detail in section IV-2-a. Since these two types of microstructure have such a diversified combination of properties, it is convenient initially to correlate the mechanical properties developed in this study to these two basic microstructural groups. The microstructure classification in Table 7 is based on the predominant phases observed by optical microscopy (see Figures 12 and 13).

(2) General Microstructure-Properties Relationships

The basic property trends of lenticular versus equiaxed alpha structure in alpha + beta titanium alloys are summarized in Table 8.

TABLE 8: Property Correlation to Alpha Morphology

Property	Lenticular		Equiaxed
	Coarse	Fine	
YS	low	highest	high
UTS	low	highest	high
E1	low	low	high
RA	low	low	high
FT	high	low	low

It could be seen from Table 8 that the equiaxed alpha structure is generally good for tensile properties; coarse lenticular structure is good for fracture toughness; and fine lenticular structure shows both poor elongation and fracture toughness, but good tensile strength.

(3) Microstructure Property Relationships

(The microstructure designations used here are based on Table 7)

(a) Yield Strength

As predicted from Table 8, the coarse lenticular structure (Group BC in Table 7) displayed the lowest YS. Microstructures with fine lenticular alpha (Groups BF, PEF + SF, PLC + SF and PEC + SF) displayed the highest values, while microstructures containing equiaxed alpha or mixtures of equiaxed alpha showed medium strength results.

(b) UTS

The UTS results ranked almost the same as the yield strength result in relation to the microstructure [see (a)].

(c) E₁ and RA

The coarse primary alpha condition with the lowest strength showed the highest E₁ and RA (BC and BF), while all high strength conditions (containing fine lenticular alpha) showed very low ductility.

(d) Fracture Toughness

The highest FT value were observed in microstructures containing either coarse beta annealed morphology (BC), or secondary coarse lenticular alpha (PLF + SC) or coarse primary lenticular alpha (PLC).

The lowest values were observed for conditions containing fine lenticular alpha (BF, PLC + SF, PEF + SF AND PEC + SF).

(e) Summary

From the above evaluation it is clear that the general relationships observed in other alpha + beta titanium alloys (Table 8) occur in the Ti-6Al-6V-2Sn alloy.

The existence of fine lenticular alpha phase, the result of HT1, results in reduced ductility and fracture toughness. When it exists in a relatively small volume fraction (like Sample No. 2, Figure 12), it is still sufficient to degrade ductility, Table 5, Figure 15, 16, 19 and 20.

On the other hand, the coarse lenticular structures demonstrated the best fracture toughness values accompanied by relatively low tensile strength. This trend is common in most alloys, in which low tensile strength is associated with high fracture toughness. However, in titanium alloys, the coarse lenticular morphology leads into a tortuous fracture crack path which further increases the FT values.

The fine equiaxed alpha structure provides a good combination of tensile and fracture toughness properties.

SECTION IV

CONCLUSIONS

This work has demonstrated that through use of various titanium alloy powder sources, compaction methods, and heat treatment conditions, it is possible to produce a wide variety of microstructural conditions and concomitant mechanical properties in the Ti-6Al-6V-2Sn alloy.

The properties which were of special interest in this work were tensile strength, elongation and fracture toughness. Based on previous work it was known that optimization of the properties required break-up of the continuous grain boundary alpha. A range of microstructures were produced in Hydride-Dehydride and Rotating Electrode Powder compacts using a combination of hot isostatic pressing, extrusion and isothermal forging in combination with two heat treatments. Within the range of microstructures produced, it is difficult to identify one type of microstructure which has the best overall mechanical behavior. However, two types of microstructures were identified as having adequate combinations of tensile strength, elongation and fracture toughness.

(a) The first type of microstructure has a high volume fraction of fine equiaxed primary alpha in a matrix of finely transformed beta, the result of extrusion and heat treatment (HT1) both in the alpha + beta phase field. This microstructure is known also to have good fatigue crack initiation resistance. In general, HT1 provided a large increase in tensile strength, over 20 ksi, with some loss in ductility and minor changes in toughness.

(b) The second type of microstructure has a combination of relatively coarse secondary alpha plates and a small volume fraction of large, low aspect ratio primary alpha. This microstructure can be obtained by heat treating either the hot isostatically pressed (HIP'd) or isothermally forged (IF) powder compacts in the alpha + beta phase field (HT2). This microstructure is a duplex type structure with the good fracture resistance contributed by the lenticular colony regions and good elongation contributed by the low aspect primary alpha regions. The HIP'd compacts have more coarse lenticular alpha and, therefore better fracture toughness while the IF material has more low aspect ratio primary alpha with higher ductility. There is a small reduction in yield and ultimate strength, 5 ksi average, with this heat treatment.

REFERENCES

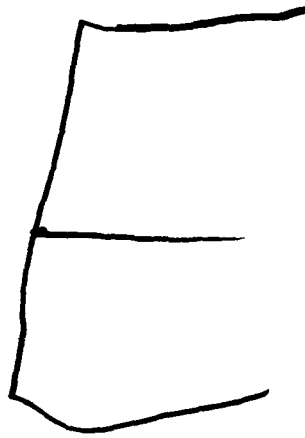
1. H.B. Bomberger and F.H. Froes, "The Melting of Titanium," *Journal of Metals*, Vol. 36, No. 12, December 1984, p.39-47.
2. F.H. Froes and H.B. Bomberger, "The Beta Titanium Alloys," *Journal of Metals*, Vol 37, No. 7 (July) 1985.
3. F.H. Froes and D. Eylon, "Powder Metallurgy of Titanium Alloys - A Review," to be published in the Proceedings of the 5th International Conference on Titanium, Munich, West Germany, 1984.
4. Summary of Air Force/Industry Manufacturing Manufacturing Cost Reduction Study, U.S. Air Force Technical Memorandum, AFML-TM-LT-73-1, January 1973.
5. J.N. Fleck and L.P. Clark: SAMPE Qtly, (October 1976) 10.
6. G.I. Friedman: Inter. J. of PM, 6 No. 2 (1970) 43.
7. G.H. Gessinger: "Titanium '80. TMS-AIME (1980) 243.
8. F.H. Froes and J.R. Pickens: J. of Metals, 36 No. 1 (1984) 14.
9. F.H. Froes, D. Eylon, G.E. Eichelman, and H.M. Burte: J. of Metals, 32 No. 2 (1980) 47.
10. C.A. Kelto, B. Kosmal, D. Eylon, and F.H. Froes: J. of Metals, 32 No. 8 (1980) 17.
11. F.H. Froes and J.E. Smugeresky, eds.: "Powder Metallurgy of Titanium Alloys," TMS-AIME (1980).
12. F.H. Froes and D. Eylon: "ASM Metals Handbook, Powder Metallurgy," 9th Edition, 7 (1984), in press.

REFERENCES - Continued

13. F.H. Froes, D. Eylon, and G.I. Friedman: "ASM Metals Handbook, Powder Metallurgy," 9th Edition, 7 (1984) in press.
14. F.H. Hayes, H.B. Bomberger, F.H. Froes, L. Kaufman, and H.M. Burte, "Advances in Titanium Extraction Metallurgy," Journal of Metals, Vol. 36, No. 6, June, 1984, P. 70-76.
15. K.H. Roll: "Progress in Powder Metallurgy 1982," MPIF(APMI. 38 (1982) 1.
16. J.A. Vaccari: American Machinist, Special Report 754, (1983) 121.
17. F.H. Froes and D. Eylon, "Titanium Net-Shape Technologies," TMS-AIME Publications, Warrendale, PA, 1984, pp. 1-299.
18. H. Jones: "Rapid Solidification of Metals and Alloys," The Institute of Metals, Monograph No. 8 (1982).
19. H. Jones: J. Mat. Sci., 19 (1984) 1043.
20. Gerald Friedman, "Development of Hot Isostatic Pressing Techniques for Producing High Quality Billet from Titanium Alloy Powder," Technical Report AFML-TR-75-9, Contract F33615-73-C-5092, April, 1975.
21. J.C. Chesnutt and F.H. Froes, "Effect of Alpha-Phase Morphology and Distribution on the Tensile Ductility of a Metastable Beta Titanium Alloy," Met. Trans., Vol. 8A, June 1977, pp. 1013-1017.
22. R. P. Simpson, C. M. Pierce, K. C. Wu, "Microstructure Control in Welding of The Ti-6Al-6V-2Sn Alloy," Titanium Science and Technology, Proceedings of the Second International Conference on Titanium, Cambridge, MA, 1972, R.I. Jaffe and H. M. Burte, Editors, Plenum Press, New York, 1973, pp. 553-571.

REFERENCES - Continued

23. F.H. Froes, "Synthesis of CORONA 5 (Ti-4.5Al-5Mo-1.5Cr)," *Journal of Metals*, Vol. 32, No. 5, 1980, p. 57-64.
24. I. Weiss, G.E. Welsch, F.H. Froes, and D. Eylon, "Mechanisms of Microstructure Refinement in Ti-6Al-4V Alloy," to be published in the Proceedings of the 5th International Conference on Titanium, Munich, West Germany, 1984.
25. I. Weiss, G.E. Welsch, F.H. Froes, and D. Eylon, "Modification of Alpha Morphology in Ti-6Al-4V by Thermomechanical Processing," to be published in *Metallurgical Transactions A*.
26. F.H. Froes, J.C. Chesnutt, C.G. Rhodes, and J.C. Williams, "Relationship of Fracture Toughness and Ductility to Microstructure and Fractographic Features in Advanced Titanium Alloys." *Proceedings of ASTM Symposium on Toughness and Fracture Behavior of Titanium Alloys*, ASTM STP 651, 1978, pp. 115-113.
27. R. Omlor, D. Eylon and F.H. Froes, an unpublished work, 1979-1980.
28. D. Shechtman and D. Eylon, "On the Unstable Shear in Fatigue of Beta-Annealed Ti-11 and IMI-685 Alloys," *Metallurgical Transactions A*, 9A (1978), pp. 1018-1021.
29. D. Eylon, J.A. Hall, C.M. Pierce and D.L. Ruckle, "Microstructure and Mechanical Properties Relationships in the Ti-11 Alloy at Room and Elevated Temperature," *Metallurgical Transactions A*, 7A (1976), pp. 1817-1826.



D T / C

7 - 86